ADVANCED ENERGY & SUSTAINABILITY RESEARCH
Open Access
www.advenergysustres.com

Carbon-Based Textile-Structured Triboelectric Nanogenerators for Smart Wearables

Abdullah Sayam, Md. Mahfuzur Rahman, Abu Sadat Muhammad Sayem, A. T. M. Faiz Ahmed, and Shah Alimuzzaman*

Recent advances in wearable electronics have been propelled by the rapid growth of microelectronics and Internet of Things. The proliferation of electronic devices and sensors relies heavily on power sources, predominantly batteries, with significant implications for the environment. To address this concern and to reduce carbon emissions, there is a growing emphasis on renewable energy harvesting technologies, among which textile-based triboelectric nanogenerators (T-TENGs) stand out as an innovative and sustainable solution due to having the interesting characteristics like large contact area, lightweight design, flexibility, comfort, scalability, and breathability. T-TENGs can harness mechanical energy from human movement and convert it into electric energy. However, one of the challenges is low electric power output, which can be addressed by meticulous selection of material pairs with significant differences in work function and optimizing contact areas. The incorporation of carbon-based nanomaterials, such as carbon nanotubes and graphene, emerges as a key strategy to enhance output. This review delineates recent progress in T-TENGs incorporating carbonaceous nanofillers, comprehensively addressing fundamental classification, operational mode, structural design, working performance, and potential challenges that are hindering commercialization. By doing this, this review aims to stimulate future investigations into sustainable, high-performance smart wearables integrated with T-TENGs.

1. Introduction

With the advent of technologies like wireless sensor networks and the Internet of Things (IoT),[1,2] the number of wearable devices is increasing every day. As a result, the demand for miniaturized power supply sources is also on the rise. Generally, batteries are used to power these devices. However, there are concerns about the negative effects of batteries on the environment because of the harmful chemicals they contain. Consequently, the weight of batteries makes wearable devices feel heavy, which can cause a negative sensation or discomfort on users' skin. Additionally, batteries have a short lifetime and a negative cost impact on users due to recurring purchases and difficulties in recycling.[3–6] Nanogenerators (NGs) are being suggested as the reliable and sustainable alternatives to batteries in this regard.

A nanogenerator is an amazing novel technology that converts thermal or mechanical energy, generated from small scale physical movements, into electricity. There are different types of NGs such as triboelectric nanogenerators (TENGs), piezoelectric nanogenerators (PENGs), and pyroelectric nanogenerators (PyNGs). Their energy harvesting mechanisms are also different. For instance, a PyNG collects energy from a thermal source, whereas TENG and PENG scavenge energy from a mechanical source.[7–11] Apart from these energy harvesting NGs, there are various wearable harvesting systems such as biofuel cells, solar cells, and so on. However, they all are associated with distinct limitations (see **Table 1**).

A TENG, a nascent technology, can capture intermittent mechanical stimuli, especially low-frequency (<5 Hz) movements of humans, and convert this low-frequency mechanical energy into high-frequency sustainable electric power based on triboelectrification and electrostatic induction. They are frequently used for

A. Sayam
Department of Textile Engineering
Ahsanullah University of Science and Technology
Tejgaon, Dhaka 1208, Bangladesh
E-mail: sayambutex@gmail.com

The ORCID identification number(s) for the author(s) of this article can be found under https://doi.org/10.1002/aesr.202400127.

DOI: 10.1002/aesr.202400127

M. M. Rahman
Department of Industrial and Production Engineering
Bangladesh University of Textiles
Tejgaon, Dhaka 1208, Bangladesh

A. S. M. Sayem
Manchester Fashion Institute
Manchester Metropolitan University
Manchester M15 6BG, UK

A. T. M. F. Ahmed, S. Alimuzzaman
Department of Fabric Engineering
Bangladesh University of Textiles
Tejgaon, Dhaka 1208, Bangladesh

Table 1. Classification and limitations of different energy harvesting device.[37,43,48,187,188]

Classification	Energy source	Energy harvesting device	Limitations
Nonrenewable	External power source	Rigid battery Lithium-ion battery	Bulky system is incongruous for the skin, predominantly originates from various toxic chemicals, short life span, poor electrical capacitance, the prerequisite of frequent charging, costly disposal process, threat to the ecological balance, overcharging poses flammability threat
Renewable	Mechanical energy	Piezoelectric nanogenerator	Limited scopes of material choice, high impedance, unreliable mechanical durability, strain-dependent structure which causes lower output power, difficult to integrate with textile as intermittent alternating current (AC) input needs to convert in direct current (DC), requires continuous movement of the object, lower efficiency (0.01–21%)
		TENG	Requirement of frictional contact reduces the mechanical lifespan of the TENG device, some stacked structures are susceptible to delamination failure, inferior working stability, operation temperature is constrained by electron thermion emission, movements with several degrees of freedom are difficult to harvest, output performance heavily relies on input frequency
	Thermal energy	Thermoelectric generator	Impossible to use during a cloudy day or at night due to dependency on temperature gradient, higher output resistance, complex configuration, low output voltage, limited number of materials available for selection, low conversion efficiency (0.1–25%)
		Pyroelectric nanogenerator	Susceptible to temperature fluctuation, constrained material selection, pulsed AC as input
	Magnetic energy	Electromagnetic generators	Cannot capture low frequency motion, occupies large space, impaired by heavy weight and rigid texture dependent on coil and magnet, complex structure, short range transmission of power
	Solar energy	Solar cell	Nonfunctional in the absence of sunlight, heavily dependent on the surrounding environment
	Biomass energy	Biofuel cells	Require auxiliary catalysts that are not available regularly, low efficiency, prohibitive cost

different on-body electronics applications.[12–14] The technology is functional in multiple operating modes that are biocompatible, cost-effective, and flexible materials. Their manufacturing route is not arduous, and the performance of the technology can be further tweaked by different surface modification techniques. The advantages of TENG are illustrated in **Figure 1**.

The quest for suitable materials to get the best electrical output from TENG has been a long going effort. In the beginning, most of the materials used were primarily polymer and metal based. Although textiles primarily originated from polymers, raw polymers possess low stretchability and flexibility, insignificant air permeability, limited maneuverability, and hence inconvenience to the wearer.[15] Applying these substrates for harnessing biomechanical energy was thus impeded. To encounter these issues, the inception of textile-based TENGs (T-TENGs) came to light. However, their application is cumbered by lower output.[16,17] In this regard, T-TENGs incorporated with carbonaceous substances like carbon nanotube (CNT), graphene, and graphene derivatives present an auspicious prospect. T-TENGs have already emerged as a topic of interest for many researchers.[18–21] However, to the best of our knowledge, no review article on the performance of carbonaceous nanomaterial-incorporated T-TENG for smart wearables has come out. Published literature has thoroughly reviewed different low-dimensional carbon nanomaterial-based nanogenerators.[22,23] But symbiosis between textile and carbon material-based TENG has been overlooked so far. This article unravels the authentic relationship between textiles, carbon materials, and TENG. The review focuses on electrical performance, durability, washability, applications, and special attributes of T-TENGs and classifies carbon-based nanogenerators according to their fabricated textile structure. It also identifies the weakness in constituent materials and proposes a trajectory for future research that is expected to play a guiding role in the development of smart textiles of the future.

2. Overview of T-TENG Technology

2.1. Construction of TENG and T-TENG

TENG, first introduced by Z. L. Wang in 2012,[24,25] converts mechanical energy into electricity during frictional interaction between two different triboelectric materials having dissimilar electron affinities connected by electrode utilizing the contact electrification and electrostatic induction effect.[26–31] The output electric current produced by this mechanism is irrevocably pertinent to Maxwell's displacement of the current equation.[32,33] For this reason, this nanogenerator is highly efficient in terms of performance. But TENG still suffers from low power output and poor sensing ability. T-TENG dispels this problem by fully utilizing the internal space of the textile structure to increase the contact area between triboelectrification layers.

Electrode is a key constituent for any TENG. Metal-, carbon-, or polymer-based materials are preferred as electrode materials for TENG. Although polymeric materials including polydimethylsiloxane (PDMS), polymethyl methacrylate (PMMA), polytetrafluoroethylene (PTFE), fluorinated ethylene propylene), poly(ethylene terephthalate) (PET), polypyrrole (PPy), polyamide (PA), and polyvinylidene fluoride (PVDF) are mostly used, they are not well suited for T-TENG because polymer incorporation

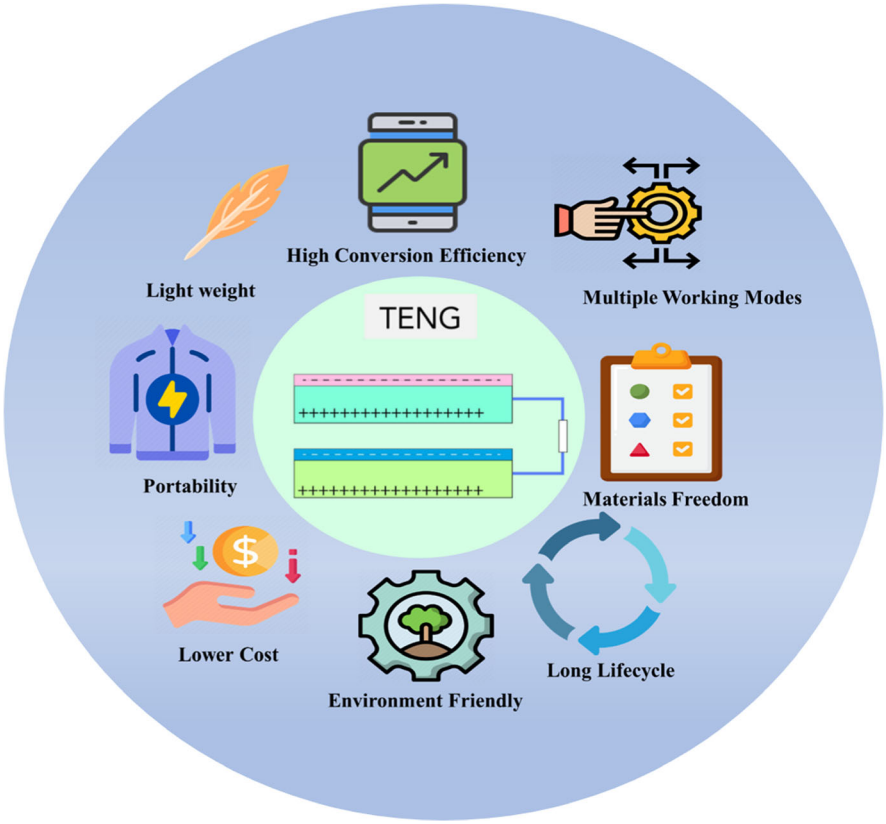

Figure 1. The advantages of TENG.

blocks porosity of the textile structure and damages inherent breathability, wearability, and comfortability of textile.[34,35] On the other hand, metal-based structures are intrinsically brittle, heavy, and susceptible to oxidation. These are incongruous with the lightweight nature of textiles because of not having sufficient stretchability and flexibility.[36] Carbon-based fillers possess nanoporous structures and are considered mechanically and environmentally superior compared to polymer or metal-based materials.[37] Carbon is a variegated material having three different hybridization phases: *sp*, sp^2, and sp^3. This leverage of bonding enables versatile geometric formation and tuning electrochemical and physical properties. Additionally, the use of carbonaceous materials like graphene, CNTs, and graphene derivatives is burgeoning rapidly due to their salient carrier mobility, high electrical conductivity, aspect ratio, and surface charge density.[38,39] Moreover, carbon nanomaterials have diversified morphologies ranging from 0D to 3D.[40] Without any doubt, nanodimensionality, surface tunability, dimensional structure, flawless electric performance, and abundant supply of these carbon nanofillers indicate their potential toward energy harvesting application[41] Latest research has also dived into the exploration of fabricating a hybridized structure combining T-TENG and supercapacitor (SC) for perpetual energy harvesting and energy storage function. In some of these works, only SC is fabricated by carbon-based materials[42] which are kept outside of the scope of this article. It focuses solely on those T-TENGs that are fabricated using carbon-based materials.

2.2. Fundamental Operation Modes

Electrostatic charges of opposite polarities are generated on the surface of triboelectric materials when two different triboelectric materials of juxtaposing polarities come close to each other, and the exchange of electrons takes place between them. For this transfer of electrons, two materials (triboelectric) must slide over each other. Through frictional contact, electric charges are separated and transferred (material to material) to establish an electrified contact which is defined as the triboelectric effect. It is to be noted that one of the two surfaces is negatively charged due to its high electron affinity while the other surface is positively charged. The way to create a potential difference between two charged surfaces is to create a distance between them which can also be created by an external force. This yields the creation of potential and a polarization-induced current. Lateral-sliding (LS), vertical contact–separation (CS), single electrode (SE), and freestanding (FS) are the four primary working modes of TENG.[43–45]

2.2.1. Vertical CS Mode

A TENG that works on CS mode is composed of two distinct triboelectric materials facing each other that contain electrodes and are deposited in opposite directions to form a stacked configuration. At least one of the triboelectric materials must behave as a dielectric otherwise it will be impossible to hold

a charge on the surface. One of the prerequisites for conducting charge toward two oppositely charged surfaces is the establishment of frictional contact between the triboelectric materials. Here, the potential difference depends on the distance between the elements. The electrical potential of the electrode is higher toward the positive surface than toward the negative surface. At the initial stage, two dielectric materials come into contact when an external force is applied to them. The triboelectric effect then causes surface charge transfer on these two interacting surfaces (**Figure 2**a.i). The opposing triboelectric charges on the two surfaces will naturally split when the external force is detached, creating an electric field and inducing a potential difference between the two electrodes. The electrons will move between two contrasting electrodes to screen this potential difference (Figure 2a.ii). This process will keep generating electricity until the potentials of the two electrodes are equal (Figure 2a.iii). Figure 2a.iv represents that the transferred charges will then begin to flow back via the external load to create another pulse of current in the opposite direction when both sheets are forced together again, causing the triboelectric-charge-induced potential difference to start to fall to zero. The generation of the AC signals will continue if this periodic mechanical deformation occurs. Transfer of electrons occurs due to potential difference, and it continues until the potential difference is equal or equilibrium. To increase the rate of electron transfer and to create a potential difference, the gap must be reduced. Elbow bending, finger pressing, and foot tapping are prime examples of vertical contact friction.[46,47]

2.2.2. LS Mode

A TENG working on LS mode plays a leading role in energy harvesting via horizontal friction utilizing sliding biomechanical movements from arm and leg swing of human body. Interestingly, LS and CS modes are almost identical in construction.[48] Figure 2b(i–iv) shows a schematic representation of the mechanism for LS mode-based electricity generation. Two triboelectric material surfaces are fully in contact in their initial position. The interaction between them will cause electron injection attributable to the two materials' unique differences in their capacity to lure electrons. There is no potential difference between the two electrodes throughout this time (Figure 2b.i). Relative displacement happens in the lateral direction as soon as the positively charged surface begins to glide outward, which is depicted in Figure 2b.ii. It is noteworthy that when the two materials are fully mismatched, the potential difference and the volume of transmitted charges have reached their maximum values (Figure 2b.iii). Figure 2b.iv displays that the transferred charges on the electrodes will flow back through the external load and provide a negative current signal to maintain electrostatic equilibrium when the top triboelectric material reverse its direction to move inward. There will not be any transferred charges left on the electrode once the two materials have fully returned to their initial location. As a result, no output current can be perceived. One thing is to be noted here, the initial aligned position of the substrates is mainly required for the electrons to return to the potential equilibrium state. AC output can be obtained when

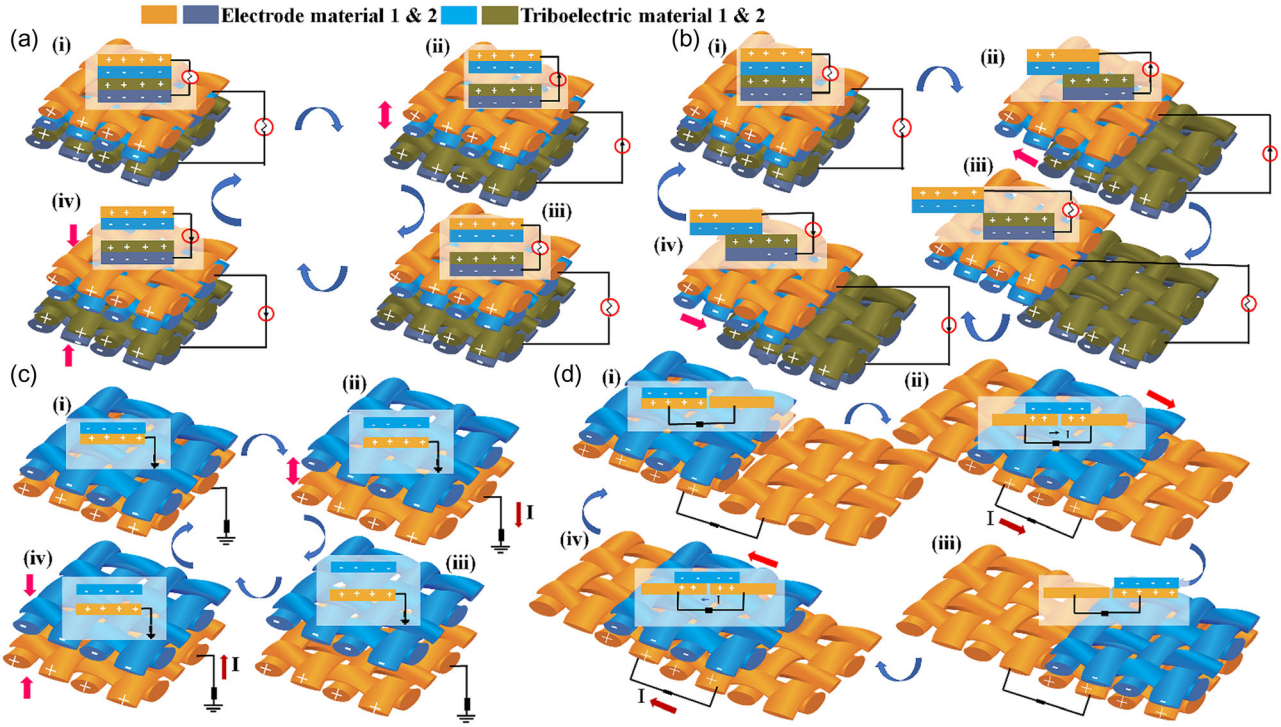

Figure 2. Four fundamental operational modes of textile-based TENGs, including a) CS mode, b) LS mode, c) SE mode, and d) FS triboelectric mode (explained in the clockwise direction).

periodic sliding occurs between the elements. Due to the greater frictional contact created by sliding, charge separation occurs, which is instrumental in bolstering the performance of the TENG. Unfortunately, the high friction is responsible for greater material abrasion. Considerably, the lateral movement of the assembly requires at least twice the area than that of CS mode. Following this issue, the T-TENG is fabricated with a linear-grating structure so that the performance of this mode increases while operating the device under the same surface area by reducing the sliding distance.[43,44,47]

2.2.3. SE Mode

In SE mode, a TENG requires only one electrode. A reference electrode is often used as a source of electrons and is attached to the primary electrode.[44,49,50] The transfer of charge between triboelectric material and human skin happens at the contact interface when they are in touch (Figure 2c.i). Human skin electrons are infused into triboelectric material. Due to the insulator's properties, the generated negative triboelectric charges on the triboelectric material plane can be maintained for a long period. A potential difference between the electrode and the grounded reference electrode is created as the human skin gets separated from the triboelectric surface. To reach an electrostatic equilibrium circumstance, as shown in Figure 2c.ii, the positive charges on the triboelectric material side will induce negative charges on the electrode. This will cause a stream of free electrons from the electrode to the ground via the external load. When negative triboelectric charges on triboelectric material virtually cancel out the generated positive charges on the electrode, an output current signal can be produced by this electrostatic induction stage (Figure 2c.iii). The free electrons drift from the ground to the electrode until the skin and triboelectric material film are fully in touch once more when the human finger turns around to face the triboelectric material again, producing a negative current signal as illustrated in Figure 2c.iv. It is noted here that this phenomenon occurs due to the occurrence of periodic vertical contact-dissociation movement in the dielectric. The primary electrode, which shields an electric field when the electrodes are very close to one another, is what causes the capacitance drop between the dielectric material and the reference electrode. This mode is very common for T-TENGS because the transfer of dielectrics occurs without electrical connections or electrodes.

2.2.4. FS Mode

A TENG on FS mode maintains a fine balance between potential charges by redistributing the charge across the pair of electrodes, which is achieved by the exposure and departure of a moving entity on the surface.[51] In the initial state, there will be net negative charges and net positive charges on the inner surface of the triboelectric material layer and the surface of the left-hand electrode, respectively (Figure 2d.i). As the triboelectric material moves from left to right, a potential difference originates between the triboelectric material and the electrodes, which causes current to flow (Figure 2d.ii). No current flows through the external force once the triboelectric material plate fully reaches the right-hand electrode's position of overlap (Figure 2d.iii). An AC is generated in the external load when the triboelectric material plate is switched to sliding backward (Figure 2d.iv). This is how power is produced in a cycle. FS T-TENG utilizes lateral body motion energy.[52] Recently, an FS mode T-TENG with a novel grated strip textile design was developed.[53] An interesting point to mention here is that the amount of voltage required to drive a digital clock can be produced by this FS T-TENG, which requires the arm to oscillate at a frequency of 2.5 Hz.

2.2.5. Comparison of Operational Modes

T-TENG can harvest different types of biomechanical energy (from the human body) for power generation by fully employing the advantages of the four modes. The critical comparison between the four operational modes is presented in **Table 2**.

2.3. Compatibility with Human Motion

The biomechanical motion of the human body is an environmentally friendly, feasible, pervasive, and sustainable solution of energy for powering on-body electronics.[54] But this motion is often intermittent, discontinuous, and hence unpredictable. This ubiquitous and abundant source of renewable energy will be a complete wastage unless otherwise utilized properly. For instance, the energy linked to biomechanical motion can be reached 67 W during walking.[55,56] TENG augments biomechanical motion into a real-time and noninvasive source of energy. During biomechanical motion, muscles are actively engaged in positive mechanical work to produce motion and negative mechanical work to subsume the energy and function as a brake to curtail the motion. Energy harvesting TENG partly substitutes the muscle activity by taking over the negative work segment for effectively converting into electricity without being any interference with the natural motion of the human body.[57] The major energy generation points of the human body are the upper limb, elbow, shoulder, ankle, knee, hip, finger, etc. **Figure 3** schematically presents the position of these limbs in the human body and the amount of energy generated by these human body parts.

Primarily, the maximum biomechanical energy originates from lower limb motion, like knee (33.5 W), ankle (18.9 W), and hip (7.2 W). The weight of the object human, the walking or running speed, frequency of the movement, angular velocity of a joint, bending angle of limbs, and contact area during motions are crucial factors that shape output electricity generation. For instance, frequency of movement during walking and running can be 1 and 3–10 Hz respectively, and alternating speeds can be 1.75 and 5 $m\,s^{-1}$.[36] Moreover, the maximum impact force of the ground reacting on the shoe is usually 1.2 times the human body weight, and right after the heel strike this heel compression occurs.[58] In addition to that, leg and arm swinging speeds are usually 1.3 and 0.8 $m\,s^{-1}$, respectively.[36] Prospectively, the output electrical attributes can also be enhanced by increasing the bending angle up to a certain threshold.[59] These parameters should be kept in mind for impeccably devising a rationally designed energy harvesting device. It is discernible from Figure 3 that lower limbs (knee, heel strike, ankle,

Table 2. Comparison of different operational modes.[37,162]

Modes	Structural characteristics	Pros	Cons	Key parameters	Application occasions
Vertical CS	Vertical upward and downward movements of triboelectric layers and electrodes with large gaps between them	High output voltage, simple fabrication process	Pulse output	Average velocity, separation distance, dielectric thickness, position of materials in triboelectric chart, operating frequency, relative humidity	Bending, tapping, pressing, vibration, impacting, sharking
LS	Sequential contact and separation mechanism without any gap, utilizes lateral polarization	Use auspicious impact of horizontal friction, provides continuous and high frequency electricity output	Requires bigger area, causes higher abrasion	Sliding velocity and distance, grating structure, operating frequency	Swinging, cylindrical rotation, disc rotation
SE	SE, bottom electrode is grounded	Straightforward integration by utilizing human skin as dielectric material. The structure can remain stationary and can be utilized as a touch sensor	Lower output performance and distorted signal	Electrode gap distance, contact area, operating frequency	Typing, sliding, touching screen
FS	Multiple styles of movements, asymmetric charge distribution, symmetric electrode	Better output performance as there is zero shielding effect, not susceptible to heat generation and material abrasion, long-term reliability, suitable for detecting moving objects	Complex integration process	Electrode gap, freestanding height, operating frequency	Vibration and rotational energy harvesting

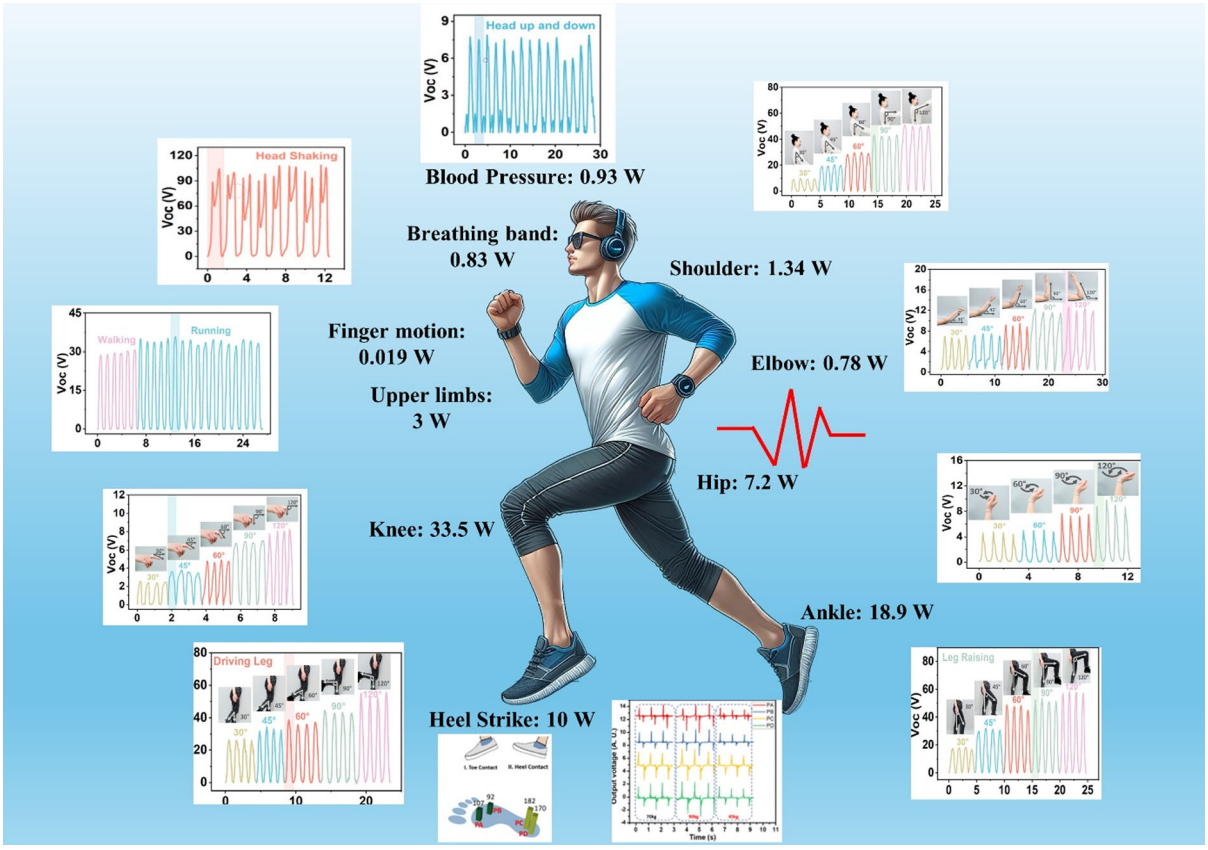

Figure 3. Schematic illustration of major energy generation points[59,179] and amount of energy generation[180,181] during everyday bodily activities of human body (V_{OC} = open-circuit voltage).

hip) generate maximum energy compared to upper limbs, elbow, and shoulder.

2.4. Compatibility with Textile

The conformity of textiles with TENG endows them with the add-on features of breathability, pliability, lightweight, and bulk production feasibility. As TENGs rely on compressive forces or stretching, and relative motion, their conformability with textiles is far better than other self-powered generating devices.[60,61] For these reasons, TENG has turned out to be a cynosure of self-powering wearable textile research and has been stated in several recent papers.[62,63] All the other nanogenerators other than TENG are handicapped by different internal and external factors which make them ineffective and unpopular for smart wearables.

TENG is always considered a better nanogenerator for integrating with textiles. Nevertheless, a TENG needs to be engineered properly for utilizing ambulatory power. Improvement of triboelectric charge density and contact area, and reduction of dielectric constant and layer thickness have an auspicious impact on output power and impedance trait. Similarly, frequency and amplitude rate, conformity of the device, and, most importantly, separation of TENG layers must be ensured for utilizing dynamic motion.[64]

3. Textile Structures for T-TENG

Textile materials have been part of human civilization from a very early age. With the progression of time, the role of textiles has become more diversified that ranging from being simple covering material to being an intelligent material that can sense, hear, respond, and bring improvisation if required.[65] Compared with other methods of wrapping, embedding, and attaching, textiles can be more efficaciously integrated with electrical functions without causing any extra burden or sullying the natural appearance of textiles.[66] Textiles are also naturally endowed with complex deformation to stress and resistance to fatigue wear. Moreover, they have excellent moisture management properties and can be utilized to cover complex curved structures.[67] Thus, textiles present a wide avenue of design inspiration and multifunctionality for TENGs. As a result, both seamless energy harvesting and superior wearing comfort are ensured in a T-TENG presenting a new research direction for smart textiles.

Textile structures are classified as 1D or multidimensional. 1D textile structure or yarn is formed by interlocking/assembling fibers with texturing, twisting, or twining along the axial direction. This 1D structure can be further morphed into 2D and 3D textile structures by employing manufacturing techniques like weaving, knitting, braiding, and nonwoven.[36] Weaving can be regarded as the interlacement of two sets of yarn at a right angle to each other. The vertical set of yarn is called warp and the horizontal set of yarn is called weft.[68] According to the pattern of interlacement, woven fabric can be classified as plain, twill, and satin structures. Woven fabrics have robust anisotropic mechanical properties and possession of large in-plane shear enables them for further 3D deformation.[69] That is why weaving has become an indispensable cornerstone for fabricating T-TENG. On the other hand, knitting utilizes one set of yarn to produce a symmetrical intermesh of loops horizontally and vertically following a tortuous path which finally yields an inherently flexible knitted structure. Owing to this, knitted fabric can be stretched in all directions and widely used as T-TENG right after woven structure.[42] Nonwoven is another form of textile structure that is created by haphazardly orienting numerous staple or filament fibers in a fibrous web. Later, the fibrous web is reinforced by thermal, chemical, or adhesive methods. Nonwoven structures have relatively less application in T-TENG due to lower abrasion resistance, durability, and strength.[70] Another basic textile structure is braiding which is created by intertwining at least three sets of yarns imparting higher strength and stiffness.[71] There is also 3D structure-based textile fabric which has a higher number of fiber arrangement layers in the in-plane direction and bonding fibers in the out-of-plane direction.[65] As a result, 3D fabric structures have better dimensional stability, pressure response, sensitivity, out of plane mechanical properties, and spatial networking which foster better electrical performance than microporous T-TENG. Additionally, 3D printing (3DP) can be utilized to produce intricate scalable 3D textile structures which provide accurate readings of voltage, current, and output power.[72,73]

Besides, the application of electrospun nanofiber-based textile structures for fabricating T-TENG has gained momentum due to their excellent breathability, massive specific surface area and aspect ratio, possession of a large number of contact sites, lightweight, and flexible characteristics.[74] They also render high surface charge density and precisely manipulate the dipole moment of different polymers by adjusting their crystal structure to attain higher electrical output. Electrospun nanofibers can further work as an impediment between two frictional layers and thus improve durability.[75] Because of these spatial features, large output efficiency can be attained by electrospun nanofiber-based TENG. Relevant research includes Jiang et al. who fabricated a TENG utilizing electrospun silk fibroin nanofiber membranes (NFMs) as positive friction layer and electrospun PVA/MXene NFM as negative friction layer.[76] According to their finding, 1087 mW m^{-2} peak power density was achieved. Another TENG structure created by Gogurla et al. sandwiched CNT between two layers of silk fibroin NFMs which yield 6 mW m^{-2} power density.[77] Yin et al. fabricated a novel all electrospun TENG where the positive friction layer was composed of polylactic acid/chitosan/aloin NFM and the negative friction layer was prepared by carbon black-incorporated polyurethane (PU) NFM which yielded flawless charge storage capacity, transfer rate, and highly durable (>7200 cycles) structure.[75] Similarly, Yin et al. fabricated an electrospun hybrid NFM structure comprising PU/carbon black nanofibers and polyvinylidene fluoride-*co*-trifluoroethylene (PVDF-TrFE) nanofibers which were combinedly used as a negative triboelectric layer.[78] PU/carbon black NFM effectively constrained the delamination of PVDF-TrFE and as a result better output performance of TENG was observed (**Figure 4**).

4. Different Carbon-Based Materials for T-TENG Fabrication

Carbon-based nanofillers are widely pervasive on earth due to their distinguishable surface area, thermal and chemical stability,

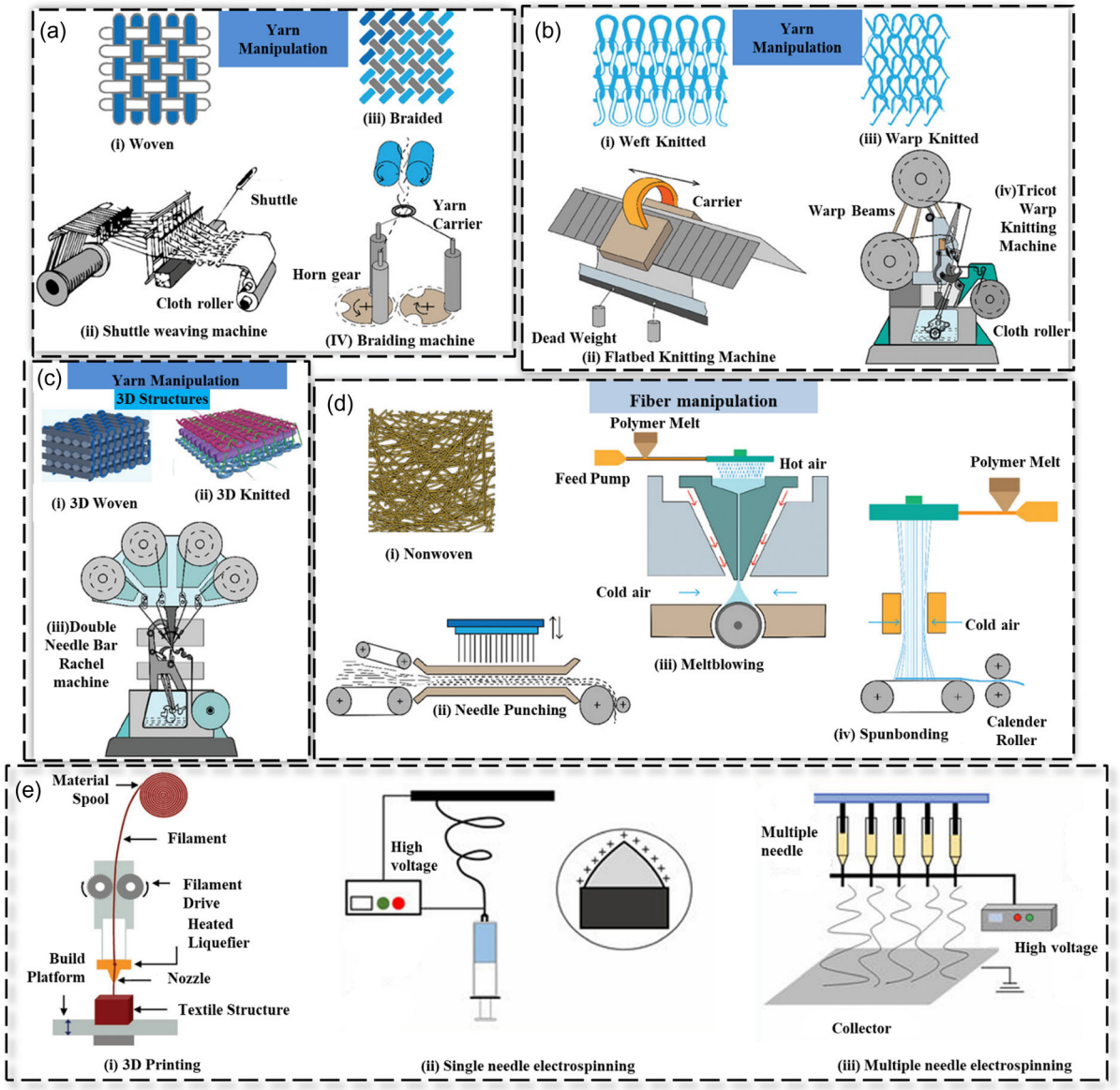

Figure 4. Summary of the distinct textile structures of woven, braided, knitted, 3D fabric, nonwovens, and related fabric production technology. a) Woven and braided structures: i) interlacement of yarns at right angle creates woven structures, ii) in shuttle weaving machines, iii) intertwining of yarns creates braided structures, and iv) in a braiding machine. b) Weft- and warp-knitted structures: i) interlooping of yarns crosswise constructs stretchable weft-knitted structures, ii) in flatbed knitting machines, iii) interlooping of yarns lengthwise creates warp-knitted structures, and iv) in tricot warp knitting machines. c) 3D fabric structures: i) 3D woven, ii) 3D-knitted structures, and iii) the 3D-knitted fabric is manufactured in a double needle bar raschel machine. d) Nonwoven structures: i) nonwoven structures are formed by directly manipulating fibers; different primary nonwoven manufacturing processes, such as ii) needle punching, iii) melt-blowing, and iv) spunbonding technologies.[182] e) Modern 3D printed and electrospinning nanofiber structure: i) 3D printing by fused deposition modeling. Reproduced with permission.[183] Copyright 2020, Wiley. ii) Electrospinning by single needle and iii) electrospinning by multiple needle. Reproduced with permission.[74] Copyright 2023, Taylor and Francis.

lighter density, low cost, variegated form, and astounding electrical conductivity.[79,80] Despite being biocompatible, flexible, and deformable, the application of most T-TENGs is cumbered by low electrical output. The desired triboelectric performance can be achieved by augmenting the capacity of charge trapping and reducing the internal impedance through the application of different low-dimensional carbon nanofillers like CNT, graphene, graphene oxide (GO), reduced GO (rGO). Their high electrical conductivity, large surface area, flawless mechanical and optical property, anticorrosion durability, and inherent carrier mobility make them ideal constituents for large-scale production of T-TENG.[23,81] **Figure 5** depicts different nanodimensional (0D to 3D) carbon nanoparticles (NPs) widely used in T-TENG and their advantageous traits.

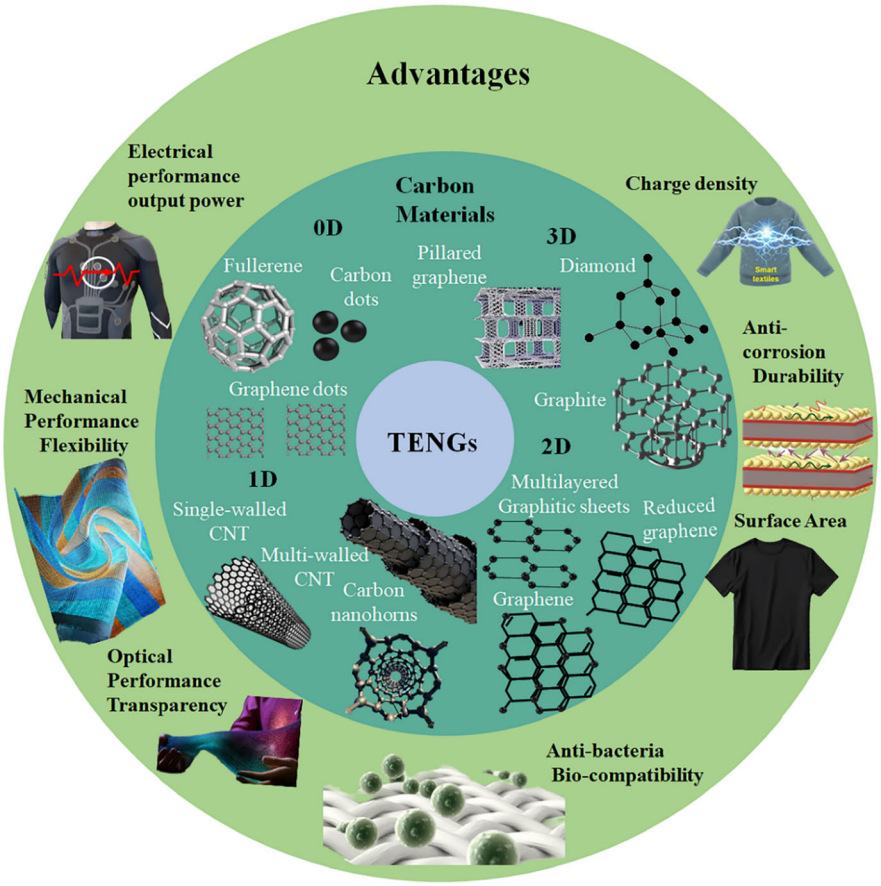

Figure 5. Different low-dimensional carbon NPs for T-TENG and their advantages.[23]

4.1. Graphene

Graphene is a carbon material, which has drawn the attention of the scientific community in recent years. After the confirmation of C60 fullerene structure in 1989, followed by the invention of CNT in 1991, graphene discovery in 2004 by Novoselov et al. challenged the stereotypical understanding of structure and properties of 2D carbon-based materials.[82] Graphene is a hexagonal 2D honeycomb crystal structure which is originated from a highly dense monolayer of carbon atoms and occupies sp^2 configuration in the atomic structure.[83] Kim et al. suggested the world's first graphene-based flexible TENG for energy harvesting at the year of 2014.[38] Graphene is different from all other nanomaterials due to its mechanical, electrical, and thermal properties including astounding mechanical flexibility and elasticity, ultrahigh electron mobility, and extraordinary thermal stability.[84] Surprisingly, although graphene is the thinnest nanomaterial (thickness of 0.34 nm), it retains more strength than steel and at the same time remains highly stretchable and conductive.[85] Also, it is worth mentioning that Young's modulus of graphene is 1100 GP.[86] Besides higher conductivity, graphene incorporation improves the capacitance, increases the electron trapping sites, and abates the dielectric loss. These phenomena combinedly bolster TENG's performance. Surprisingly, when multiple graphene sheets are stacked one over another, the structure may turn into highly flexible and conductive graphite. As graphene obstacles the diffusing and drifting of electrons due to intrinsic densely packed aromatic sp^2 hybridized structure, graphite paper endows with electron blocking capability.[81] Additionally, graphene naturally contains many ripples in the structure due to the inhomogeneous interaction with substrate which further galvanizes the surface roughness and contact area.[87]

4.2. GO

Low impurity graphene production requires costly fabrication methods which are often commercially not feasible. GO, which is derived by oxidation of graphene, appears to be a competitive substituent. The myriad of oxygen functional groups in the structure enables its dispersibility into water and many other solvents which ease the fabrication process and lower the cost.[88] Because of these diversified functional groups (carboxyl, hydroxyl, etc.), graphene nanosheets can be deposited on arbitrary substrates, unveiling their potential application in energy harvesting.[89] The abundance of oxygen functional groups enables GO with strong negative charge trapping capability which alongside staggering surface area makes GO an ideal constituent for T-TENG.[90]

4.3. rGO

The rGO can be produced by thermal, chemical, or electrochemical reduction of GO.[91] Generally, it possesses less oxygen content compared to GO. Their electrical properties are not analogous to graphene and can be modified by manipulating the functional groups of oxygen.[92] Interestingly, rGO can be prepared in any quantity by different fabrication methods like photoassisted, microwave, and thermal. What mostly makes rGO compatible with TENG is its extraordinary conductivity and superior mechanical stability. Researchers have also found rGO efficacy in resolving electrostatic induction hindrance and surface charge decay issues.[48,93] The rGO additionally modulates interfacial energy band alignment which improves the electron trapping ability and hence higher triboelectric performance can be achieved.[48]

4.4. CNTs

CNTs, which were first reported in 1991 evidently by rolling up graphitic sheets into 1D tubular form, are composed of either only one graphitic wall or of several coaxial tubes of graphene layers. They are known as single-walled CNT (SWCNT) and multiwalled CNT (MWCNT), respectively.[23] CNTs have an astounding aspect ratio (length to diameter ratio), staggering surface area, high electrical conductivity, exceptional specific stiffness, spatial hollow cylindrical topography, low surface tension, a hydrophobic trait, and convenient surface modification provision.[22,94] All these factors foster better triboelectric performance.

4.5. Fullerene

Fullerene is a 0D structure having highly symmetric and nonpolar carbon molecules.[95] Fullerene exerts a positive impact on tribology applications attributed to its lubricating behavior. The spatial spherical morphology produces robust intermolecular bonding which is conducive for further surface medication. Furthermore, the absence of high energy vibration between different bondings in the structure renders high applicability to T-TENG.[95,96]

4.6. Graphene Quantum Dots

Graphene quantum dot (GQD) is a 0D material originating from 2D graphene.[97] GQD possesses graphene lattice inside the dots, which are ten layers thick and 100 nm in size. The properties of GQDs can be modulated according to the specific requirements of diversified applications. Due to the intrinsic structure, GQDs manifest special edge and quantum confinement effect. As a result, electron distribution is significantly altered within the crystal boundary. Additionally, GQDs exhibit higher energy spectral due to nonzero bandgap, and have better solubility, surface grafting, nontoxicity, and biocompatibility compared to other carbonaceous nanofillers. The electrical properties of different carbonaceous materials are shown in **Table 3**.

4.7. Carbon-Based Composite

Incorporating MXene with conductive polymers ameliorates the performance of T-TENG. MXenes, such as transition metal carbides, carbonitrides, and nitrides nanosheets, are emerging as promising 2D nanomaterials, primarily because of their outstanding metallic electrical conductivity.[98] With terminating functional groups containing oxygen and abundant fluorine groups, MXenes are triboelectrically more negative than PTFE, making them suitable as negative triboelectric materials in TENGs. MXene has an auspicious impact on polymer crystallinity, dielectric properties, surface charge density, and electrical conductivity.[81] Mxene–PTFE active layer can lead to 6 and 4 times improvement of current and voltage, respectively, compared to sole PTFE triboelectric negative layer.[99] Moreover, the adaptation of MXene/PDMS composite film as the triboelectric negative layer leads to 7 times enhancement of output voltage and current compared to pristine PDMS TENG.[100] Incorporation of MXene significantly improved the electron trapping ability and decreased the interfacial impedance of the TENG structure. As a result, the tribonegativity had drastically increased. MXene was also incorporated with PVA hydrogel, resulting in higher stretchability stemming from cross-linking nature.[81] Simultaneously, Mxene also improved ionic transport and conductivity resulting in higher output of TENG. Furthermore, TENG originated from MXene/PVDF composite obtained 1.6 times pick power density than raw PVDF nanofibers

Table 3. Electrical properties of different carbonaceous materials.

Materials	Diameter [nm]	Aspect ratio	Surface area [$m^2 g^{-1}$]	Electron mobility [$cm^2 V^{-1} s^{-1}$]	Electrical conductivity [$S cm^{-1}$]	Specific conductivity [$S m^{-1} g^{-1} cm^{-3}$]	Resistivity [Ω cm]	Current density [$A cm^{-2}$]	References
CF	7300	440	0.7	–	–	–	2.0×10^{-3}	–	[189,190]
SWCNT	0.6–0.8	10 000	415	20–10 000	5000	0.5×10^{6}	10^{-6}	10^{7}	[189,191]
MWCNT	12.5	8000	≈165.6	–	11 200	4×10^{6}	5×10^{-6}	10^{4}–10^{5}	[189,191]
Graphene	10	35 000	2630	26 000	10^{6}	–	1.19×10^{-6}	–	[189,192]
GO	1.2	3200	≈2391	–	–	–	21.87×10^{-6}	–	[189,193]
RGO	–	–	–	–	103.3	–	23.73×10^{-3}	–	[189,194]
Carbon black	15–300	20–50	–	5.4	10^{6}	–	–	–	[22,189,195,196]

stemming from electrostatic interaction between the functional group of MXene and PVDF polymer.[101] Jiang et al. devised a TENG utilizing electrospun PVA/MXene NFM as a negative friction layer and achieved 1087 mW m^{-2} peak power density.[76] Bayan et al. fabricated a T-TENG that incorporates an active layer composed of silver (Ag) NPs loaded onto graphitic carbon nitride (g-C3N4) nanosheets on carbon fibers.[102] They demonstrated that this composite material could generate an open-circuit voltage reaching ≈200 V and charge a commercial capacitor to around 85 V within only 30 s.

5. Constituents of Carbon-Based T-TENG and Their Impact on Triboelectric Performance

The role of triboelectricity in influencing the performance of TENG is undeniable as it plays a major role in creating the surface charge effect. It should be noted here that the smooth formation of triboelectric charges is essential for generating the desired current and voltage. Charge density can be significantly increased by enhancing its surface area with the help of nanostructures and nanopattern materials. Another novel method of increasing it is the use of charge-trapping additives and charge-transporting layers within insulating triboelectric materials.[22,23] Researchers are now increasingly leaning on 2D carbonaceous materials in addition to 1D carbonaceous materials. The main motivation behind this is their remarkable properties such as high conductivity, flexibility, transparency, stretchability, lightweight, and high surface-to-volume ratio. These properties are auspicious for triboelectric performance. As a result, the widespread application of different low-dimensional carbonaceous materials like graphene, CNT, GO, and rGO either in triboelectric materials or in electrodes is easily observable.

5.1. Carbonaceous Triboelectric Materials

Triboelectrification is the frictional surface charging effect between two triboelectric materials during their contact and separation. Therefore, the selection of triboelectric materials exerts a crucial role in determining the output of the T-TENG. Triboelectric effect can be produced between two different kinds of materials or sometimes by two chemically same materials having nonhomogeneous surface properties.[81] The polarity of triboelectric materials is at the forefront of output performance of TENG, swayed by work function and electron affinity of that particular material.[37,48] Triboelectric polarity can be understood from a triboelectric series, which is sorted according to the material's intrinsic tendency of losing or gaining electrons. The topmost materials of the chart will be triboelectrically positive and further descending into the chart, material becomes triboelectrically negative. Thus, using two materials with further distance apart in the triboelectric series will maximize the performance output.

Before the invention of TENG, Park et al. discussed a triboelectric series based on various plastic materials.[103] This triboelectric chart was supplemented by Zou et al. who summarized triboelectric chart based on the versatile class of materials.[104] Following this, Hatta et al. more exhaustively analyzed different triboelectric materials and ranked them according to their triboelectric charge density.[105] However, at first, it was considered that planar membranous construction does not represent highly deformable and porous textile structure. For this purpose, Liu et al. measured the tribocharge densities from 21 widely used textile fibers by sliding mode triboelectrification.[106] The charge density of textiles can be effortlessly measured under fabric densification phase when triboelectrification reaches its saturation point.[107] It appeared that there was not much discrepancy between the results of complex hierarchical structure and planar membranous structure. Therefore, it was concluded that triboelectric series representing film materials is also applicable to textile materials.[106] The study also identified effective surface area as the most critical structural characteristic of textiles for measuring triboelectrification performance compared to other characteristics (frictional coefficient, compressibility, surface roughness). Hence, it can be said that carbon fiber and other low-dimensional carbon-based materials find their efficacy as triboelectric material in TENG structures predominantly for large surface areas.

5.2. Carbonaceous Electrode Materials

It is evident in various studies that electrodes can greatly influence the performance of T-TENG. Any inferior electrical characteristics of the electrode including low carrier mobility and density can result in a downgraded efficiency of TENG. Regarding the selection of electrodes, metal electrodes are less durable, and they are also not compatible with textiles as they lack stretchability and breathability and to some extent even susceptible to failure from cyclic bending.[108] A more rational approach is polymer-based electrodes which also lack compatibility with porous fiber and complex geometrical structures.[109] Besides, polymer-based electrodes naturally possess less conductivity.[48] So, the electrodes should be redesigned because there is no chance to underestimate the role of electrodes in energy conversion. In this regard, carbon-based electrodes are considered best due to their high conductivity, flexibility, stretchability, hydrophobicity, washing resistance, and improved chemical, mechanical, and electrical stability.[22] **Figure 6** presents an ideal wearable electrode's key performance factors which are all checked by a carbon-based electrode.

Additionally, carbon-based materials can also be coated on metal electrodes to substantiate the electrostatic induction effect. For instance, copper is prone to oxidation which occurs at room temperature and causes damage. In 2020, Yang et al. reported a more preferable approach to prevent the oxidation of copper electrodes by graphene dispersion which was fabricated by spin coating.[110] Chu et al. presented a SE TENG structure that was based on chemical vapor deposition (CVD) grown atomically thin graphene (<1 nm).[111] Yang et al. fabricated the graphene electrodes by spin coating the conductive polymer PEDOT:PSS (PH-1000) on the transferred graphene.[108] Graphene dispersion ameliorates the charge collecting capability of electrodes.[112,113] Besides graphene, CNTs are the most widely used electrode for mass scale fabrication of T-TENG.[109] For fabrication, dipping and drying method is widely used for incorporating SWCNT or MWCNT in T-TENG structure.[110]

Laser-induced graphene (LIG) is produced by exploding and synthesizing a carbon source, and this synthesis is done by

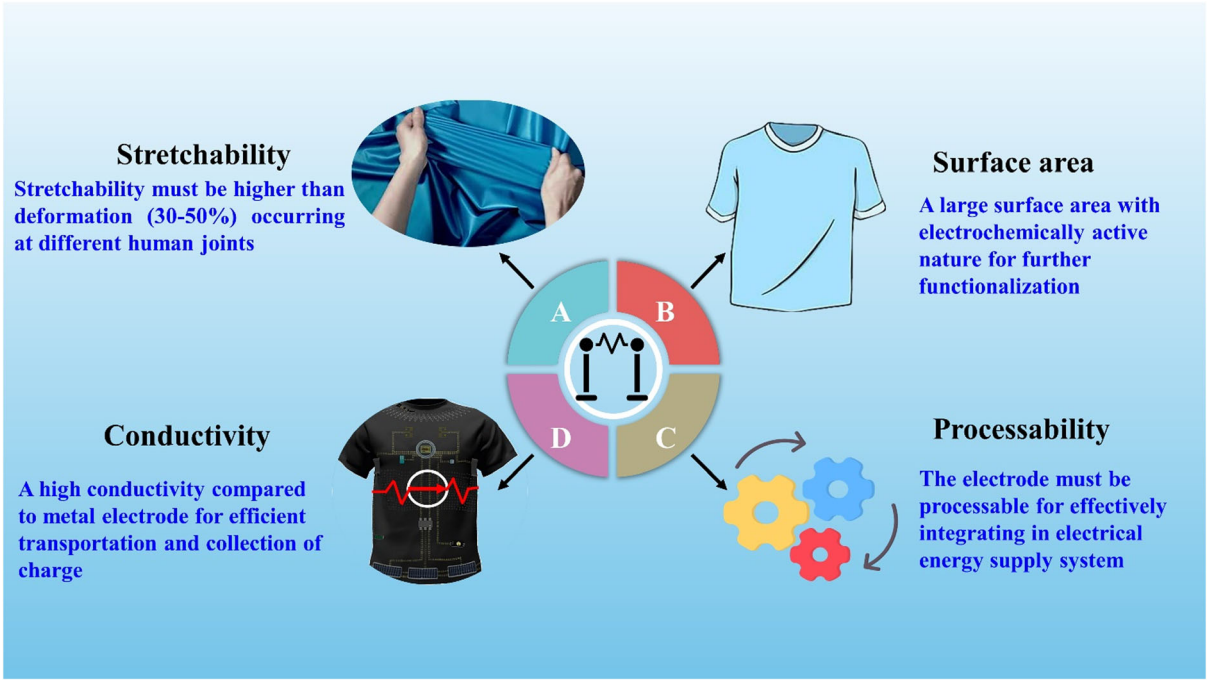

Figure 6. Key factors of an ideal wearable electrode.[184]

carbon dioxide laser. This LIG is a graphene-like material. The conversion of sp^3 carbon to sp^2 and the removal of noncarbon ingredients is performed by pulse laser irradiation which is a photothermal process. The production of TENG by LIG electrodes is gaining popularity day by day because it has certain properties that distinguish it from others, such as high conductivity, good physical strength, and thermal and chemical stability.[114,115] Thus, graphene and its derivatives, CNTs, fullerenes, diamonds, activated carbons, etc. play a crucial role in fabricating T-TENG. Between all these materials, CNT translates better electrical performance in structure because of having robust structural interaction and a more aligned structure. On the contrary, graphene fibers are advantageous for their facile, low-cost fabrication method.[116]

6. Classification of T-TENG Based on Geometrical Structures

Based on the review of contemporary literature, T-TENGs can be classified as a) fiber- and yarn-based T-TENG and b) fabric-based T-TENT according to their basic textile structures. Further, they can be subclassified into different categories according to their textile geometry which are elaborated in the following subsections.

6.1. Fiber- and Yarn-Based TENG

1D fiber-based TENGs can be readily integrated with conventional textiles because of their advantageous nature in terms of extensibility, deformability, washability, compactness, and breathability.[117] They are functional under multidirectional forces and appear to be more reliable for long term usage. Their classifications are described below.

6.1.1. Entwined Fiber-Based T-TENG

Zhong et al. shed light on a fiber-based TENG that converts vibrational energy and biomechanical motion into electricity by electrostatic induction.[118] Built upon an entwined structure principle, these fiber-based TENGs are made of CNT-coated cotton thread (CCT), and PTFE and CNT-coated cotton thread (PCCT). Both threads were entwined in a double-helical configuration (**Figure 7**a). CNTs strongly adhere to the cellulose surface due to their intrinsic nature of chemical bonds. The double helical structure can either be kept in linear form (Figure 7b) or converted into a curvy shape (Figure 7c) due to the intrinsic flexibility of the structure. This twisted fiber-based TENG can be later woven into fabric (Figure 7d) to devise a "power shirt" for wireless temperature monitoring purposes. Figure 7e demonstrates a simplified circuit of fiber-based generator based on CS mode. PTFE is known as the most electronegative material in the triboelectric series and can hold static charges on its surface for a long time. Through oxygen plasma treatment, the accumulated charges can be sustained for more than 20 days resulting in greater longevity of the device. Simultaneously, CNT in both CCT and PCCT would accumulate positive charges on the surface. Consequently, change in interfiber gape distance between PCCT and CCT would result in accumulation of positive charges on the CNT layer of CCT which later unobtrusively flow toward CNT layer of PCCT to balance the electrical field. Due to stretching and releasing function, an AC output signal will be generated via CS principle and the device always returns to its original

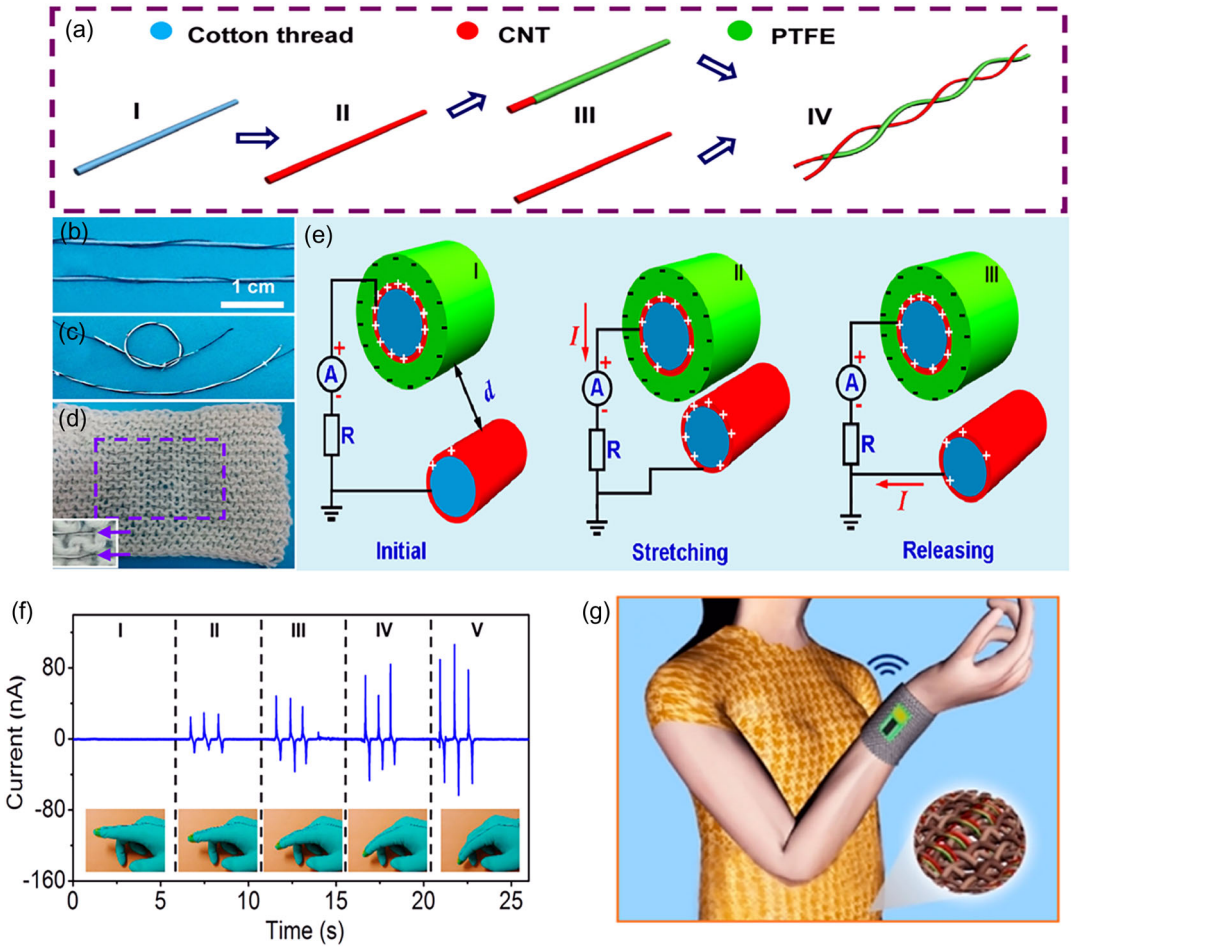

Figure 7. a) Schematic diagram of fiber-based generator based on entwined structure principle; magnified photo of NG with b) linear shape, c) curved shape, and d) woven into fabric; (e) schematic diagram of power generation mechanism of fiber-based NG; f) current–time response curve of self-powered active sensor for body motion detection; and g) schematic diagram of wireless body temperature sensor system triggered by the "power shirt." Reproduced with permission.[118] Copyright 2014, American Chemical Society.

shape denoting high flexibility. This device could produce an average out power density of 0.1 μW cm^{-2} which is applicable to active body motion detection. As Figure 7f depicts, those five different motions of index finger fixed with TENG produced different output currents. The "power shirt" can be actively engaged as a wireless temperature monitoring system (Figure 7g) by proper integration with capacitor, microcontroller, and other electronic equipment.

6.1.2. Coaxial Fiber-Based T-TENG

Coaxial structure fiber is another fiber-based TENG in which two different materials are exposed to each other but separate within a single fiber structure. Coaxial structures have better stretching and bending performance than entwined double-helical structures. The very first coaxial structure consisted of Al, PDMS, and nanowires with nanotextured surfaces.[119] This spatial structure ensured increased contact area and higher flexibility of TENG which yield higher output. Carbon material-based TENGs are also readily fabricated by this orientation. Yang et al. developed a carbon material-incorporated TENG based on the coaxial structure principle which was latter integrated with a SC.[120] Here, carbon fiber bundles were employed as electrode material for higher conductivity and capacitance behavior and silicone rubber was used as both triboelectric and encapsulation material for TENG and coaxial fiber, respectively. As can be seen from **Figure 8**a, carbon fiber electrode materials were first wrapped around the SC which was based on H_3PO4/PVA electrolytes. Later, silicone rubber encapsulates this structure. The TENG functions according to SE principle and charges are accumulated on silicone layer (Figure 8b). The measured diameter of the coaxial fiber was just 2 mm. This unique coaxial structure performs remarkably well during enwinding, bending, and knotting which is prerequisite for smart wearable textile fabrication. The highest output power generated was 1.12 μW at a motion frequency of 2.5 Hz (Figure 8c). In addition to that, Zhang et al. proposed a fiber-based coaxial-structured TENG where CNT ink acted as core electrode material and silk fibroin and PET were chosen as triboelectric pair (Figure 8d).[121] The pattern was then 3D printed on conventional

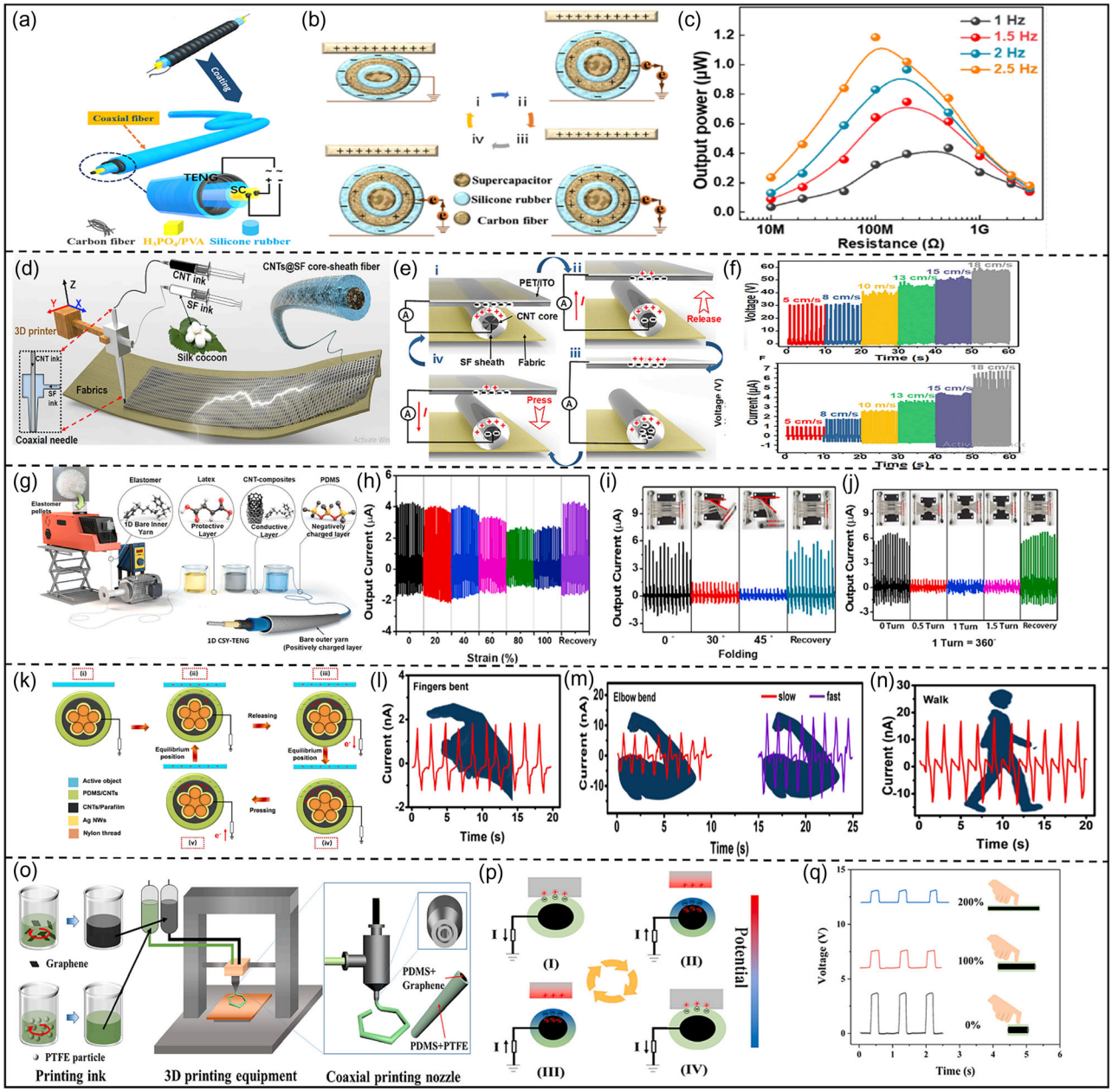

Figure 8. a) Fabrication process of coaxial fiber TENG integrated with supercapacitors, b) working mechanism of the TENG in the SE mode, and c) output power of the single fiber of TENG under different operational frequency. Reproduced with permission.[120] Copyright 2018, American Chemical Society. d) Schematic illustration of 3D printing process utilizing a coaxial spinneret, e) working mechanism of smart textile, and f) output voltage and current on the textile while contacting/separating with a PET film at different displacement speeds. Reproduced with permission.[121] Copyright 2019, Elsevier. g) Schematic fabrication illustrations of CNT-incorporated 1D coaxial stretchable yarn TENG. Output current of stretchable yarn TENG at different h) strain%, i) folding angle, and j) twisted state. Reproduced with permission.[123] Copyright 2022, Elsevier. k) SE working mechanism of triboelectric sensor based on combined triboelectric and piezoelectric effect. The current signals of the yarn TENG under l) finger bending, m) elbow bending, and n) walking. Reproduced with permission.[124] Copyright 2022, Elsevier. o) Schematic diagram of the 3D printing process of coaxial stretchable smart fiber involving graphene, p) SE mode of producing triboelectric effect, and q) comparison of the voltage signal of the fiber with different tensile strain under the same press force. Reproduced with permission.[126] Copyright 2021, Elsevier.

fabric for harnessing mechanical energy from human movement. The working principle of this T-TENG based on CS mode is described in Figure 8e. PET has a strong affinity to receive electrons and silk has a strong tendency to dispatch electrons via CNT ink-based electrodes, resulting in a greater triboelectric effect. It was also evident that changing displacement velocity from 5 to 18 cm s^{-1} results in increased output current and voltage to 7 μA and 55 V, respectively (Figure 8f). The achieved

output power density by this core–sheath structure was around 18 mW m^{-2}. The TENG was mechanically sustainable as the structure can withstand 15 000 cycles of loading/unloading. Furthermore, Yu et al. fabricated a coaxial-structured TENG employing CNT sheets as outer and inner electrode material and PDMS and PMMA as triboelectric pair.[122] Introduction of micropores (5 μm) in the triboelectric structure resulted in the surge of roughness and contact area which yields 130% and 150% improvement of current and voltage, respectively. The porous structure can respond to multidirectional mechanical stimuli (compression, vibration, stretching, bending, twisting) without any cracks.

Moreover, Kim et al. fabricated a spatial FS 1D coaxial TENG endowed with the capability of morphing into versatile geometrical orientations under stretching or twisting.[123] Here, CNT composite layer along with latex and PDMS was used for dip-coating bare inner yarn where PDMS acted as the triboelectric negative element and bare outer yarn acted as triboelectric positive element (Figure 8g). The fabricated device remained refractory against stretching, deforming, and impairment by water. The maximum output voltage did not flinch even after 6000 cycles demonstrating the superior stability of the structure. Figure 8h–j reveals a decrease of output current from 4.25 to 2.75 μA at 100% strain, 6.06 to 0.9 μA at 50% folding state, and 6.56 to 1 μA under 1.5 turns, respectively. But all these outputs of scalable array coaxial stretchable yarn TENG retain their original performance after recovery denoting their flawless power generation property despite being stretched, twisted, and folded. In addition to that, Yan et al. reported a rare coaxial fiber TENG based on SE mode (Figure 8k) for recognition of gesture where CNT-based composite was coated on the silver nanowires and elastic nylon-based conductive electrode to realize flexible and elastic coaxial fiber which was later applicable as textile-based triboelectric sensor.[124] This type of T-TENG is unlike to change at 150% tension and can be easily knitted, folded, or reversed into various convenient shapes. The hierarchical structure is built upon a rough surface morphology that can be attributed to the irregularly stacked CNTs composite cluster. This rough surface ensures a conductive percolation system with multiple pathways for transporting charge which subsequently results in high stability and deformability of the core conductive electrode. The sensor builds upon this principle can later detect finger bent (Figure 8l), arm bending (Figure 8m), and measure the actual number of footstep completed during walking (Figure 8n). Additionally, novel polycation-modified carbon dot-incorporated PVA matrix found their efficacy in fabrication of nanocomposite polymer electrolytes (NPEs) which latter can be transformed as NPEs fiber.[125] Following this, core–sheath-structured NPE–TENG is fabricated which is endowed with phenomenal electrical output (265.8 μW m^{-1}) predominantly arising from high dielectric constant. This higher dielectric output is achieved by fostering ionic conductivity through modification of functional carbonaceous nanofillers. Other than that, the structure maintains good washability and mechanical stability which are paramount for wearable textiles. Besides these, 3DP technology can be used to fabricate a core–shell structure whose core is filled with graphene and PDMS and shell is occupied by PTFE and PDMS, respectively (Figure 8o).[126] The incorporation of graphene modulates the rheological properties of PDMS and improves the conductivity and sensitivity. Graphene has a high aspect ratio which augments the strength of PDMS matrix by forming conductive web pathways. Figure 8p demonstrates the working principle of this TENG in SE mode while utilized as a tactile sensor. The fiber-based TENG was attached with a copper wire for signal acquisition. There was a direct analogy between contact pressure and electric signal of TENG. The efficacy of this TENG as a tactile sensor was validated by decreasing voltage signal from fiber stretching (Figure 8q). Stretching yields reduction of fiber diameter and hence reduced contact area.

6.1.3. Wrinkled Fiber-Based T-TENG

Another type of coaxial fiber-based TENG is reported for its increased stretchability due to added wrinkle layer which is known as wrinkle-structured TENG. Sim et al. employed MWCNT fabricated by CVD method as outer electrode of stretchable triboelectric fiber with wrinkle structure at outer surface.[127] This type of TENG is more adaptable for body parts with high strain such as knee joints, fingers, and elbows. At first, a stretchable electrode based on PU fibers was wrapped by nylon 6,6 yarn coated with Ag. Later electrospinning method was used to fabricate highly triboelectrically negative PVDF-TrFE material with a diameter of 750 nm. Finally, CNT outer electrode was used to wrap the stretched structure at 180% strain. Due to the nonelastic nature, PVDF-TrFE will absorb this large strain of 180% by aligning haphazardly oriented nanofibers at the initial stretching direction. As a result of this, upon releasing the strain, CNT and PVDF-TrFE will combinedly form uniform and tightly packed wrinkles in a multilayered core–shell structure (**Figure 9**a). CNT showed excellent conductivity by robustly adhering to the PVDF-TrFE. Here, Ag and CNT worked as two electrodes and PVDF-TrFE and nylon/PU functioned as two triboelectric materials and generated electricity based on CS method (Figure 9b). As the distance between the electrodes increased, the electric output power also increased.

Moreover, Chen et al. fabricated a wrinkle-shaped TENG through porous carbon/PEDOT:PSS-based materials.[128] The output efficiency of the structure was propelled by increasing the carbon concentration. The higher output performance can be attributed to increased contact area. The structure was extremely stable which was compatible for various wearable electronic textiles. The PEDOT:PSS@porous carbon was spin-coated on prestretched plasma-treated Ecoflex substrate. Upon releasing this prestrain, the carbon-based structure transforms into a wrinkled form. This wrinkled structure acted as both triboelectric material and electrode in fabricated TENG in pair with PTFE as other triboelectric material and gold as other electrode (Figure 9c). Plasma treatment is liable for improvement of surface adhesion which enables packing of carbon more densely. As a result, plasma-treated PEDOT:PSS@porous carbon structure-based TENG can observe an increase of 17% in output voltage and 15.30% in output current to raw PEDOT:PSS-based TENG (Figure 9d). Another perk of carbon deposition is increased surface roughness which also increases the output performance. Additionally, the wrinkled structure TENG sustained an increase of output performance up to 100% strain and 5000 stretching cycles conforming device performance and durability.

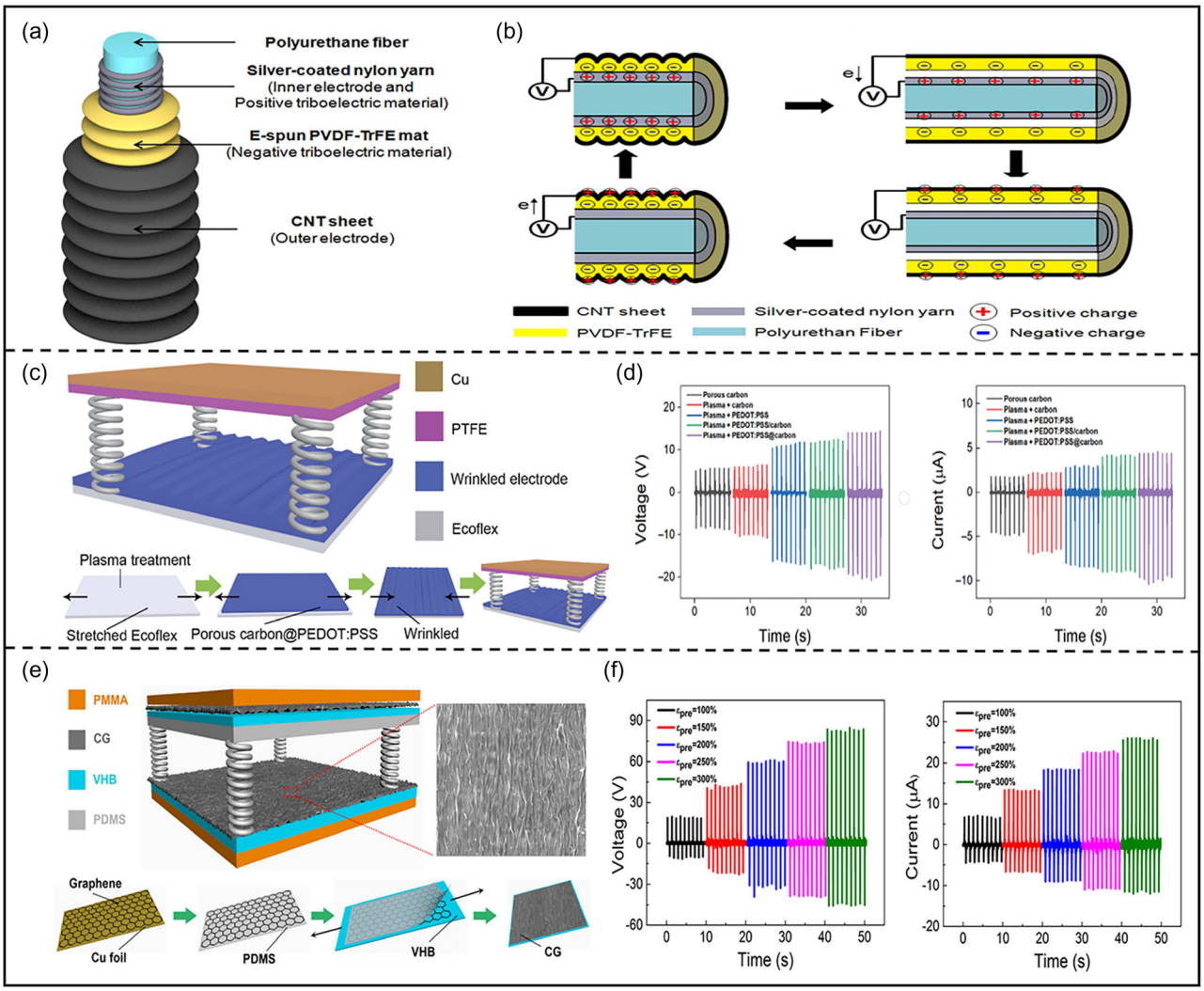

Figure 9. a) Stretchable triboelectric fiber structure and morphology and b) electrical energy generation process of stretchable triboelectric fiber. Reproduced with permission.[127] Copyright 2016, Nature. c) The fabrication process of wrinkled TENG based on crumpled PEDOT:PSS/porous carbon electrode and d) comparison of output voltage and current with other condition. Reproduced with permission.[128] Copyright 2022, Springer Nature. e) The fabrication process of wrinkled TENG based on CG electrode and f) output voltage and current at different crumple degrees. Reproduced with permission.[130] Copyright 2019, Elsevier.

Similarly, crumpled rGO-based T-TENG showed sharp increase in electricity conductivity of TENG.[129]

Interestingly, according to another study by Chen at al., the higher crumple degree has an auspicious impact on triboelectric performance.[130] They devised a flexible crumpled graphene (CG)-based TENG where two triboelectric materials (PDMS and CG) were connected by four springs which act as spacers to manipulate the gap distance (Figure 9e). As the crumpled degree enhanced from 100% to 300%, the output voltage and current increased from 18.7 V and 6.66 μA to 83 V and 25.78 μA, respectively (Figure 9f). The surface roughness, contact area, and work function difference are pivotal factors for the improvement of output performance by stretchable 2D CG electrodes. Moreover, it was validated that power density surged 20 folds when utilizing CG compared to planar graphene-based TENG.

Besides, Xia et al. fabricated nanowrinkles TENG based on bimetallic hydroxide where carbon cloth was used as a substrate material.[131] The bimetallic hydroxide of copper-nickel was grown on carbon cloth by manipulating the surface morphology through altering the reaction conditions during hydrothermal method. Here, carbon cloth-based copper–nickel bimetallic hydroxide acted as a triboelectric material and was paired with PTFE. The electrical output was maximized (328 V and 36.15 μA) when nanowrinkle structures were kept in sphere shape which maximizes the surface roughness and contact area. Chandrashekar et al. fabricated an "arch-shaped" wrinkled structure flexible TENG through eco-friendly, metal etching free exfoliation of graphene imposed as both electrode and triboelectric material.[132] The ripples and wrinkles in the structure make graphene more applicable for high voltage applications.

6.1.4. Elastomeric Fiber-Based T-TENG

The elastomeric fiber-based T-TENGs are known for their higher stretchability which generally surpasses coaxial- and wrinkle-structured fiber-based TENG. A study by He et al. utilized silicone rubber as the core of the fiber.[133] CNT and polymer matrix-based conductive layer was coated on it which was used as one electrode. Following this, stretchable silicone rubber thin film, which acts as an insulating triboelectric material, was formed around this stretchable electrode. Finally, copper microwires, which act as other electrode, were wrapped around the silicone yielding a functional elastomeric fiber-based TENG (**Figure 10**a). CNT/polymer layer imparts unparallel stretchability, flexibility, mechanical stability, and electrical conductivity. In addition to being highly stretchable (Figure 10b), the fiber-based TENG also was highly bendable (Figure 10c) and twistable (Figure 10d). The good combination between CNT and matrix in the electrode ensured higher electrical conductance even with the increase of the elongation of fiber-like TENG. This statement is affirmed by surface microstructure of fiber-based TENG at both released (Figure 10e) and stretched (Figure 10f) states under 50% strain as there was no phase separation discernible. This corroborates many conductive pathways built by CNT even under large strain. Figure 10g illustrates the working principle of this fiber-based TENG based on CS method.

Furthermore, Wang et al. fabricated an elastomeric helix-belt-type TENG structure that produces impeccable performance due to the symmetrical structure which results in indifferent contact area at different directions of pressing.[134] The triboelectric layer consisted of elastomeric silicone which has strong proclivity to gain electrons and possesses excellent stretchability and flexibility in all directions. The inner and electrodes are predominantly composed of CNT and carbon black which render a high stretchability limit of 620%. CNT enlarges the contact area and improves the conductivity under high strain. Besides stretchability, this type of TENG accounts for excellent water resistance and can aggregate a high surface charge density of 250 mC m^{-2}.

Besides these tribonegative elastomeric yarns, tribopositive yarns are also widely used. One such instance is MWCNT nanomaterial-incorporated elastomeric TENG which displays flawless real-time sensitivity. It increases the output voltage from 0.97 to 3.90 V when strain is altered from 25% to 125%.[135] Here, mechanical and electrical performance were not dispensed to each other but rather delicately balanced. Besides this, carbon conductive ink, which is an amalgam of primarily carbon and graphite, was adapted as the core conductive electrode inside poly[styreneb-isoprene-*b*-styrene] (SIS) elastomeric tube-based highly flexible 1D TENG.[136] The composite of PDMS and barium titanate NPs (BaTiO3 NPs) was coated on this SIS tube to modulate the dielectric permittivity. Thus nylon 6-coated conductive Ni–Cu fabric and PDMS/$BaTiO_3$ NPs were chosen as two triboelectric pairs of this highly flexible TENG based on vertical CS principle (Figure 10h). Interestingly, the structure showed no performance degradation even after 7000 stretching and releasing cycles under 100% strain. Similarly, the T-TENG retained their original output voltage (Figure 10i) and output current (Figure 10j) even under harsh conditions (twisting, 30 min washing, 100% stretching, folding). Because of these characteristics, this T-TENG can be used as a self-power-driven human knee protector (Figure 10k).

6.1.5. Miscellaneous Fiber-Based T-TENG

Besides these regular methods, there are also some exceptional methods for fiber-based TENG fabrication. Su et al. devised a TENG fabrication method involving electrospinning and electrospraying of CNT and silk.[137] After electrospinning of thin constituent of silk fibers, CNT-silk layer was electrosprayed on this electrospun silk layer, yielding a conductive fiber-based TENG. Having a special layered microstructure, the fiber-based TENG was extremely flexible and easily compatible with textiles. This method effectively broke the barrier of difficulty of equipping a TENG with excellent softness and higher tensile strength while maintaining biodegradability, elasticity, stability, and uniformity. In the structure, CNTs are entangled with silk fibers to occupy the nanoscale gaps. The highest power generation output was 317.4 μW cm^{-2} which is more than sufficient for driving nanoscale devices like humidity thermometers.

6.2. Fabric-Based Structures

Fabric-based structures also have diversified applications in T-TENG fabrication. Fabric-based T-TENGs have the advantages of higher output efficiency, rapid prototyping, and large contact area.[37] Their classifications are described below.

6.2.1. 3D Fabric T-TENGs

3D fabric T-TENGs are developed based on the in-plane sliding mode to avoid the requirement of air gap or spacer between the triboelectric layers. Besides, through this mode of operation, energy can be harnessed during the swinging motion of arms while running, walking, sprinting, or a cool-down walk.

Jung at al. produced a 3D T-TENG could scavenge mechanical energy during the friction between the torso and arm (**Figure 11**a).[15] Two TENGs were fabricated by patterning on carbon fabric with polyimide (PI) and PU, and with PDMS and aluminum, respectively (Figure 11b). Later, both TENGs were integrated with a symmetrical fabric-based SC which finally produced a 3D wearable TENG (WTENG) with no spacer between the triboelectric layers. Here, CNTs, which act as electrode, were synthesized on carbon fabric through CVD method. The deposition of CNTs maximizes the surface area which is conducive to higher flow of electricity. At a speed of 1.5 Hz, the WTENG-based textile structure could generate output voltage of 33 V (Figure 11c), rectified current of 0.25 μA (Figure 11d), output power density of ≈0.18 μW cm^{-2} with the leverage of harnessing both vertical and horizontal friction simultaneously. This higher output efficiency of the structure does not skew at a strained condition of 135° bending and 70 kPa external pressure which allows the device to be used as a pervasive self-powered wearable human motion monitor at multifarious states like stretching, walking, running, sprint, etc. (Figure 11e). Furthermore, Wu et al. fabricated a T-TENG based on textile/Ag nanowires/graphene that emulates in-plane sliding mode and is capable of harnessing mechanical energy induced by

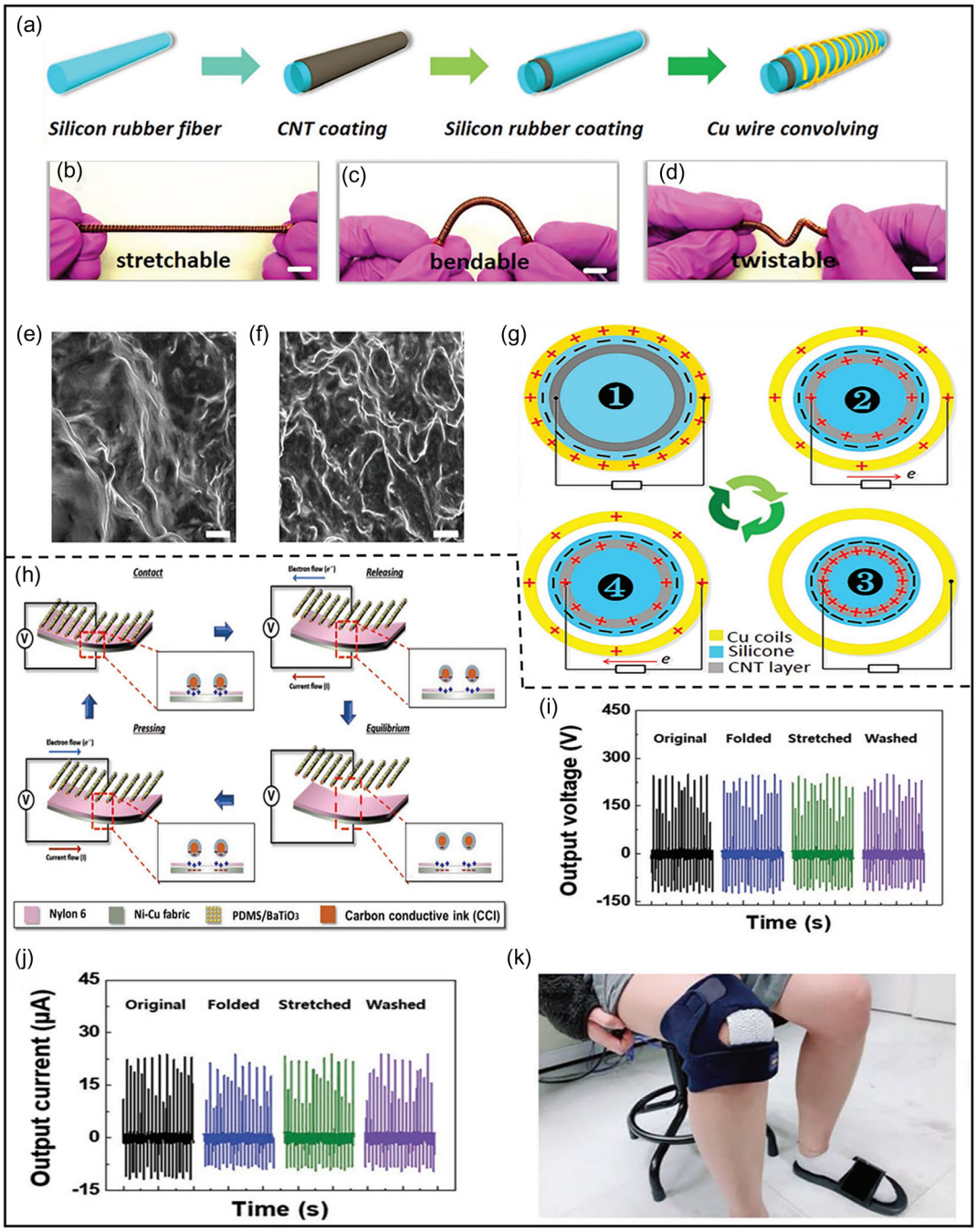

Figure 10. The structure schematic of silicone rubber, CNT, and copper wire-based elastomeric fiber-like TENG: a) fabrication process of the fiber-like TENG; the digital images of the fiber-like TENG at b) stretched state, c) bent state, and d) twisted state; zoomed-in images of the fiber-like TENG at e) released state and f) stretched state; g) the basic electricity generation mechanism of the fiber-like TENG based on CS principle. Reproduced with permission.[133] Copyright 2016, Wiley-VCH. h) Working mechanism of CCI-based TENG under repeated contact separation process, i) output voltage, and j) output current after different extreme deformation conditions; k) fiber TENG-based human knee protector. Reproduced with permission.[136] Copyright 2020, Wiley-VCH.

low-frequency friction.[138] Here, polyester yarn was used as the textile-based substrate which enables the nanogenerator to be firmly compatible with clothing. Although Ag nanowires coating is attributed to higher conductivity, this preliminary structure still fell short of mechanical and electrical stability which constraints the massive-scale production of industrial TENG. However, the deposition of GO nanosheets can turn the tide due to the inherent flexibility and large surface area of the

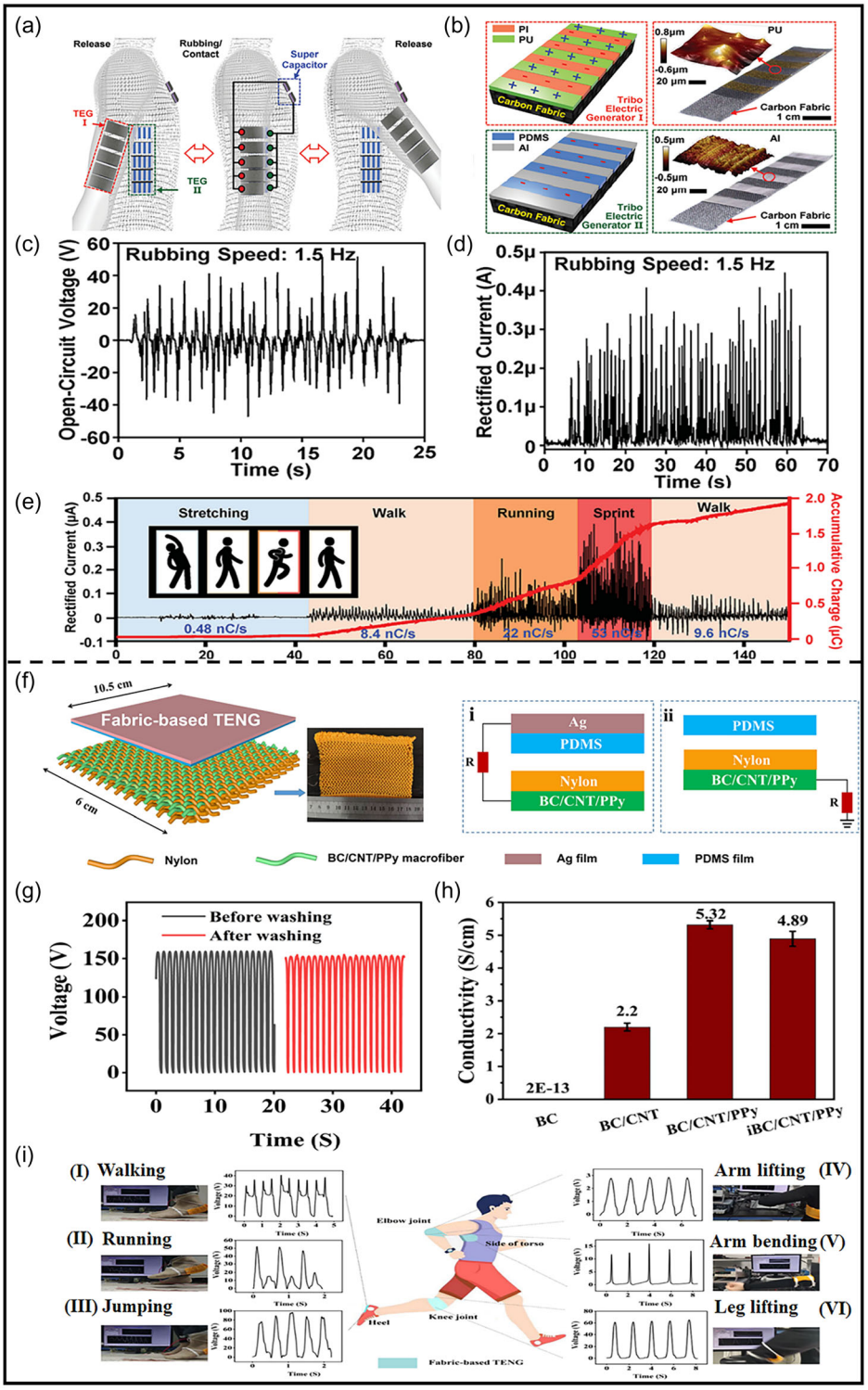

Figure 11. a) Schematic illustration of a swinging arm equipped with TENG and SC, b) schematic illustrations and digital photos of individual components: TEG I (top), TEG II (bottom), c) open-circuit voltage, d) rectified current originated by the TENG from arm swings, and e) feasibility of carbon-based TENG as human activity sensor. Reproduced with permission.[15] Copyright 2014, Wiley-VCH. f) Schematic diagram of fabric-based TENG structure based on BC/CNT/PPy and two working modes, g) output voltage of fabric-based TENG before and after washing, h) increment of the conductivity of macrofiber due to incorporation of CNT, i) testing photograph and output voltage signals of fabric-based TENG as self-powered sensor fixed to various parts of human body (heel, elbow, side of torso, and knee joint) to monitor mechanical motion: I) walking, II) running, III) jumping, IV) arm lifting, V) arm bending, and VI) leg lifting. Reproduced with permission.[139] Copyright 2022, Springer Nature.

graphene nanosheets which bolster the van der Waals force between the substrate and textile. The highest output power generation by this TENG was 7 nW cm^{-2}.

Moreover, Hu et al. underscored the necessity of fabricating TENG with conductive biodegradable materials without compromising robustness and flexibility.[139] For this reason, according to the principle of in-plane siding mode, a TENG was fabricated by sustainable bacterial cellulose (BC)-based macrofiber integrated with conductive nanofillers primarily CNT and PPy. Here, nylon was unified with BC/CNT/PPy structure forming a friction layer and PDMS/Ag was applied as another friction layer (Figure 11f). The fabricated TENG has a power output of 352 μW and can be utilized for sensing mechanical deformations during jumping, walking, running, arm bending, and leg lifting. After homogeneous dispersion of CNT, both roughness of the macrofibers and fiber diameter increased. This carbon material-based macrofiber structure translates excellent mechanical strength in the fabric-based TENG without compromising durability and stability. The TENG is fully degradable within 108 h and can sustain compression for more than one thousand cycles which mirrors its excellent biodegradability and stability, respectively. Moreover, the introduction of CNT yields looseness in the structure which imparts the TENG with washability property and results in negligible change of electrical performance before and after washing (Figure 11g). Additionally, incorporation of CNT imparts excellent electrical conductivity of 5.32 S cm^{-1} to the macrofiber (Figure 11h). As a result, for different movements like walking, running, jumping, arm lifting, arm bending, and leg lifting, excellent electricity of 40, 50, 90, 13, 2.7, and 60 V, respectively, was generated by fabric-based TENG (Figure 11i). Additionally, Zhang et al. employed an innovative brush coating method for developing nanopatterned CNT–PDMS coating on silver textile.[140] This in-plane sliding mode-based brush-coated TENG showed 72.65% increase of both open-circuit voltage and short-circuit current compared to conventional dip-coating method and was bestowed with excellent compatibility, implantability, and durability. Similarly, Shi et al. fabricated an in-plane sliding mode-based TENG employing CNT as electrode which can be later used as a smart patch for active status monitoring during walking, running, or standing.[141]

6.2.2. Multilayer Stacked 3D T-TENG

Fabrication of multilayer stacked 3D TENG (ML-TENG) is advantageous for its faster and simpler bulk production nature in addition to higher energy generation activity. This method primarily involves the employment of conductive fabric onto the commercial textile substrates.

Different carbon-based materials happen to be found in their application in ML-TENGs. For instance, Cao et al. fabricated a washable electronic textile utilizing CNT as an electrode.[142] In this ML-TENG structure, triboelectric layer of silk fabric was positioned over nylon fabric substrate with arrays of CNT electrodes working as middle layer positioned in between (**Figure 12**a). The human skin effectively worked as a second frictional layer. As a result, the ML-TENG could generate electric signals when pressed with a finger (Figure 12b). Here, CNT orchestrates stellar mechanical performance during washing and folding by adhering to the nylon substrate. As a result, no properties were degraded after 15 h of immersion (Figure 12c). Besides, the performance of CNT-based electrodes showed no sign of declination even after 2000 bending cycles which is evident of higher durability (Figure 12d). Eventually, this carbon-based 3D ML-TENG provided outstanding conductivity, breathability, and reliability.

In addition to that, Feng et al. booted the triboelectricity of a commercial pristine velvet fabric by growing hierarchical nanostructures through chemical modification of CNT and polyethylenimine (PEI).[143] In this ML-TENG structure, conductive fabrics were stacked on the backside of both pristine velvet fabric and modified velvet as current collectors (Figure 12e). The working principle was based on CS method (Figure 12f). Notably, comfort, stability, washability, and integrability with clothing were ensured along with higher triboelectric output. In this method, contact charge generation between two triboelectric pairs was enhanced by increasing the surface roughness stemming from hierarchical nontopographic structure at a reasonably low modifier chemical content. This decisive surface patterning certainly does not compromise the mechanical properties of textile substrates. When this modified velvet fabric was paired with pristine velvet, an appealing voltage of 16.3 V was recorded at a CNT–PEI concentration of 0.4 mg mL^{-1}, denoting 23.3 times improvement (Figure 12g). This is the optimal modifier concentration because any superfluous coating may cause particle agglomeration and degradation of nanogenerator property. The TENG also showed salient washability because output voltage and current decreased only 13.44 and 20.63% after 24 h of washing. Moreover, Liu et al. subvert the conventional idea of ML-stacked TENG by devising a one-step TENG fabrication method where commercially available three-dimensionally penetrated 3D spacer fabric was coated with PDMS alone.[144] Here, carbonaceous CNT sheets were stacked onto the treated fabric which worked as an electrode and silver paste acted as another electrode (Figure 12h). Most importantly, no extra patterning effect was required on the surface of the structure because ingenious holes of the textile fabric produce a rough surface upon incorporation of a CNT sheet which is instrumental for higher conversion efficiency. As a result, the electric potential of the structure was exponentially improved and bestowed with an open-circuit voltage of 500 V and peak power density of 153.8 mW m^{-2}. Moreover, due to the intrinsic nature of CNT sheet, the structure maintained integrity under bending and tremendous electrical conductivity and mechanical performance under all circumstances. The electricity generation during pressing and releasing is shown in Figure 12i.

Consequently, Bai et al. built a multilayered T-TENG utilizing flexible functional elastomeric layers and conductive fabric.[145] The spatial elastomeric layer is composed of CNTs/Ecoflex nanocomposite and low-temperature vulcanized silicone. Intuitively, the charge density and migration of these charges in TENG structure upsurge with the higher content of CNT in the structure but up to a certain point (1.6 wt%). The further increment CNT content witnesses a decline in the electrical performance of TENG due to "blocking-rejection" effect. According to this principle, the freshly accumulated charges are localized at different positions of the electrification layer and hinder the accessibility of potential newly formed charges. As a result, the accumulated charges

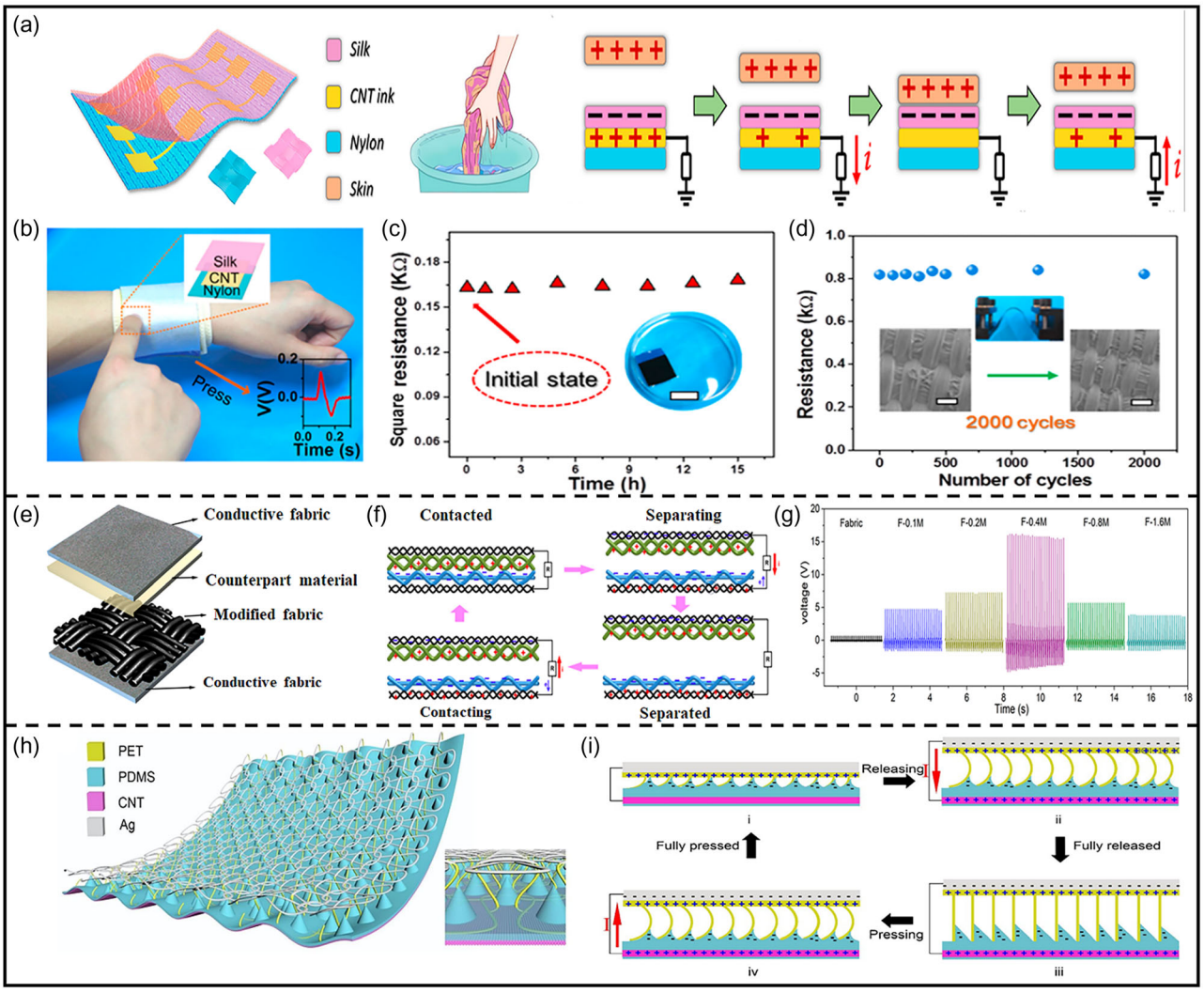

Figure 12. a) Structure design and triboelectric mechanism of the ML-TENG based on PU-CNTs ink-coated nylon fabric-based electrode and silk fabric-based triboelectric layer, b) schematic diagram of the process to generate a signal of the TENG, c) resistances of the electrode after being submerged in water for different times, and d) stability of the CNT electrode on a nylon substrate after 2000 cycles. Reproduced with permission.[142] Copyright 2018, American Chemical Society. e) Schematic of the assembled fabric-based TENG, f) working principle of fabric-based TENG, and g) output voltage results of TENGs assembled using different modified fabrics as tribopositive layer and pristine fabric as the tribonegative layer. Reproduced with permission.[143] Copyright 2021, American Chemical Society. h) Schematic illustration of the fabrication of the triboelectric textile and i) schematic illustration of the electricity generation under pressing and releasing. Reproduced with permission.[144] Copyright 2016, Royal Society of Chemistry.

reach a saturation point upon which any further inclusion of CNT renders zero impact on charge accumulation.

6.2.3. Woven 2D T-TENGs

Chen et al. fabricated a T-TENG using traditional 2D weaving principle by combining carbon, cotton wires, and PTFE.[52] The electrode of the T-TENG consisted of conductive wires of carbon was inserted through shuttle in the weft direction and nonconductive cotton thread was used in the warp direction which acted as a skeleton material of the TENG fabric. For the dielectric textile, carbon wires were used as warp thread and PTFE wires were used as weft thread. **Figure 13**a,b represents the working principle of FS T-TENG and CS T-TENG, respectively. Eventually, the fabricated TENG mimics the advantage of being lightweight, flexibility, and strong which later can be woven with SCs for further energy scavenging and storage purposes. The warp and weft thread density and diameter of carbon wires are two major parameters affecting the performance of TENG. Moreover, 80% of the original output performance can be sustained after 15 000 times repeated sliding processes. T-TENG was then attached with a pair of cotton gloves. During natural rubbing (Figure 13c) and flapping (Figure 13d) of the two gloves, the TENG experienced FS and CS modes of operation, respectively. This mechanical friction generated electricity can be utilized for powering up 18 LEDs. Speaking about carbon-based wearable electronic, cellulosic raw materials have a large skeleton of carbon structure. On the other hand, graphene is a 2D

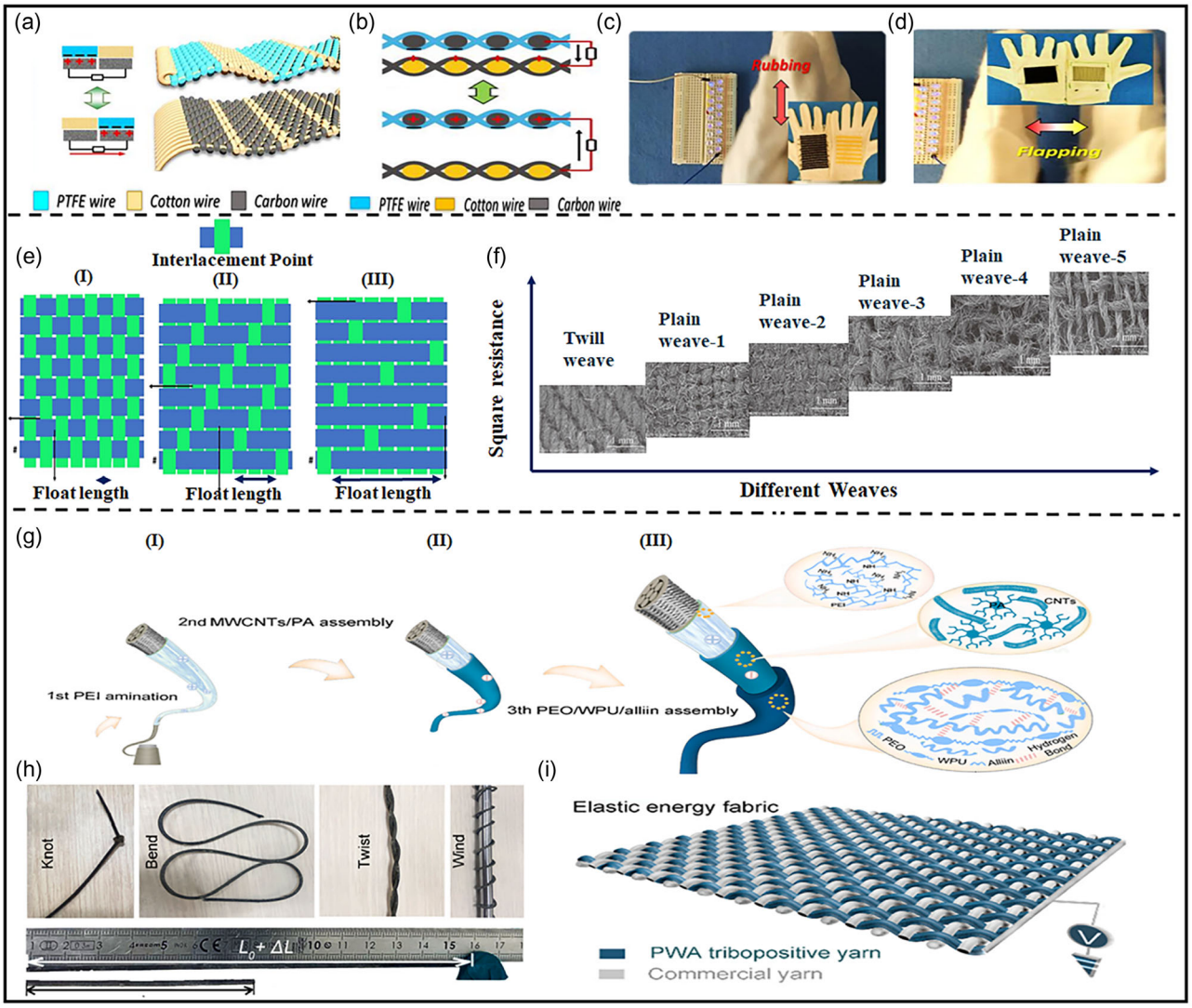

Figure 13. 2D weaving-based TENG: a) schematic illustration of the FS mode-based fabric TENG and b) CS mode-based fabric TENG. Photos of woven interlaced TENG attached onto a pair of gloves utilized for lighting up LEDs under natural c) rubbing (FS mode), and d) flapping (CS) of hands. Reproduced with permission.[52] Copyright 2018, Elsevier. e) Three basic weave structures: I) plain, II) twill, and III) satin. f) Electricity conductive performance of rGO-modified cellulosic carbon fabric for varying weave and fabric tightness.[146] g-I) PEI amination of yarn substrate; g-II) a self-assembly of MWCNTs/phytic acid layer through electrostatic attraction; g-III) PWA tribocomposite interface assembly via electrostatic attraction and hydrogen bond cross-linking interaction. h) Photographs of yarn in different deformable states including knotting, bending, twisting, winding, and stretching. i) Schematic of tribopositive yarn-based woven energy fabric as a power supply based on SE principle. Reproduced with permission.[135] Copyright 2022, Elsevier.

carbonaceous structure that is widely availed for flexible electronics fabrication purposes. Based on this, Wu et al. fabricated a rGO-modified low-cost, sustainable carbonized cellulosic fabric based on weaving principle.[146] The textile was further coated by PDMS and thus fabric-based TENG was devised. Coating with RGO certainly increases the surface roughness of the substrate which is instrumental for higher contact electricity generation. In this study, conversion efficiency of two basic weaving structures (plain, twill) was contrasted. In the weaving structure, fabric tightness factor has a direct command over surface electricity. The number of fiber interlacements and floating length in the structure are always crucial for designing a high performance woven-based fabric TENG structure. Twill structure has a longer floating length and a lower number of yarn-to-yarn interlacements in the structure compared to plain weave (Figure 13e). As a result, these structures have lowest resistance (33.3 $\Omega\,sq^{-1}$) as electrons can travel more easily compared to plain weave structures.[48] On the other hand, higher crimp of a plain weave structure makes it more convenient for flexible pressure sensors. But, as the structure possesses a higher number of interlacement points compared to twill weave, plain weave contributes less fabric surface electricity and conversely higher square resistance.

Simultaneously, square resistance is inversely proportional to the fabric tightness factor. As can be seen from Figure 13f, square resistance increased by almost 52% for loosely knitted plain weave-5 than tightly knitted plain weave-1. As a result, plain weave 1 with the highest fabric tightness will have the best electricity output performance.

In addition to that, Bai et al. devised a tribopositive yarn that simultaneously features mechanical robustness and high triboelectricity generation.[135] MWCNT was utilized as nanomaterials along with PEI and phytic acid. These nanomaterials (PEI/MWCNTs/phytic acid) were then combined with tribocomposite materials of polyethylene oxide/waterborne PU/alliin (PEO/WPU/alliin, abbreviated as PWA) to produce a novel tribopositive yarn (Figure 13g). This tribopositive yarn can withstand multiple mechanical deformations including knotting, bending, stretching, twisting, winding, and can be injected with breathability properties when morphing into fabric (Figure 13h). Later, this highly reliable, super stretchable, high power generating tribopositive yarn is weaved into the warp direction and commercial elastomeric yarn is inserted into the weft direction for devising elastic energy woven fabric (Figure 13i) which is utilized for powering up different on-body electronics.

6.2.4. Knitted 2D T-TENG

Mao et al. introduced an innovative "round tripping strategy" of knitting for devising a flexible TENG.[147] Twisted conductive carbon yarn (CCT) coated with PDMS/MnO_2 nanowire (MnO_2NW) on the surface was utilized as positive yarn and PTFE having strong electron affinity capacity was employed as negative yarn (**Figure 14**a). This round-tripping strategy subverts the conventional method as PTFE yarn knits directly closing around the conductive twisted coated carbon yarn and thus produces compressible, bendable, and WTENG. Repetitive pressing and releasing operation on this tribonegative PTFE and tribopositive CCT@PDMS/MnO_2 elastic yarn-based TENG will generate electricity (Figure 14b). It is discernible that optimum range of MnO_2NW deposition on twisted carbon yarn was 10% as any further amount of coating can cause interfacial defects and thus leakage of current instead of increasing the surface roughness for improving the output performance. The maximum output voltage and current produced by positively twisted carbon yarn were 59.6 V (Figure 14c) and 2.6 μA (Figure 14d) respectively. The TENG array textile is responsive to mechanical deformations and produces larger amount of current during jogging than walking due to the larger contact areas and closer contact made by foot stomping. Another very auspicious circular knitting technique is plating stitch-based stable knitting structure.[148] The plating stitch method imparts softness in the structure by nesting conductive and triboelectric yarn together but at the top and down surface, respectively. This delicate knitting technique increases active contact area of the structure and simultaneously ensures complex deformability, breathability, washability, and comfortability of T-TENG. But unfortunately, application of carbon-based materials based on the plating technique is overlooked and can be a prospective topic for future research.

6.2.5. 3D Knitted and Woven T-TENGs

Although 2D structures serve the purpose of complex deformation, they fall short of generating higher electrical output. On the contrary, multilayer fabric-based stacking structures with their increased contact area and thickness produce better electrical output. Unfortunately, they are also plagued by inferior integrity in the thickness direction and as a result susceptible to delamination. Contrary to all of these, 3D woven structures intertwined in x, y, z direction are better integrated.[149] Incorporation of carbonaceous fillers like CNT and GO further substantiates the career mobility, strength, and flexibility of the structure.[150]

3D-knitted T-TENG structures have lured tremendous attention due to their high permeability and elasticity. For instance, 3D spacer knitting technology-based TENG has shown great potential for energy generation devices. In this process a spacer layer which consists of spacer yarns splits bottom and top independent layers facilitating effective contact and separation for triboelectrification. For example, Zhu et al. fabricated using three sets of yarn employing computerized flat knitting machine.[151] Here, the top and bottom layers were knitted by nylon filament and the spacer layer was knitted by PET monofilament (Figure 14e). Such delicately designed spacer layer can provide unparallel resiliency to the whole fabric. It should also be noted that PET monofilament grants high stiffness and nylon multifilament provides soft handle to the fabric. In addition to that, graphene ink was used for coating the upper surface of the top layer (Figure 14f) which later actively engaged as the electrode and impart pathways for collecting and conveying the charges. Simultaneously, PTFE was chosen to coat the bottom layer (Figure 14g) for its excellent nylon compatibility and negative tribopolarity. Graphene sheets attached to the nylon surface thus ensure phenomenal conductivity of vertical contact mode-based T-TENG structure (Figure 14h). The output could be precisely tuned by controlling the number of active TENG pixels and could reach a maximum value of 16 μW. Similarly, short-circuit current also increased with the increment of number of pixels. This 3D-knitted spacer TENG effectively worked as a highly pressure sensitive sensor to quantify different types of human motions.

He et al. fabricated a 3D angle-interlock woven (3DAW) T-TENG with GO/cotton composite yarn coated with silicone rubber (Figure 14i) as warp yarn.[149] Here, GO coating on the cotton yarn acted as electrode material. Optimum output efficiencies were evaluated against the GO dipping time and silicone rubber thickness. The TENG yarn operated based on SE mode where skin was in contact with silicone and GO-cotton composited served as SE connected to the ground (Figure 14j). 3DAW-TENG structure has more interspace between the yarns and thus yields higher contact area and lower specific resistance compared to basic 2D woven structures. In the 3DAW-TENG structure, two layers of TENG yarns were used as warp yarn and four different colored z-binding yarns devised from flexible commercial stainless steel were interwoven with the warp columns and interlaced with each other simultaneously (Figure 14k). The output power of 3DAW-TENG surged to 225 $mW\,m^{-2}$. This T-TENG can be used as self-powered sensor for carpet signal monitoring from human stimuli (Figure 14l). Without any shred of doubt, it

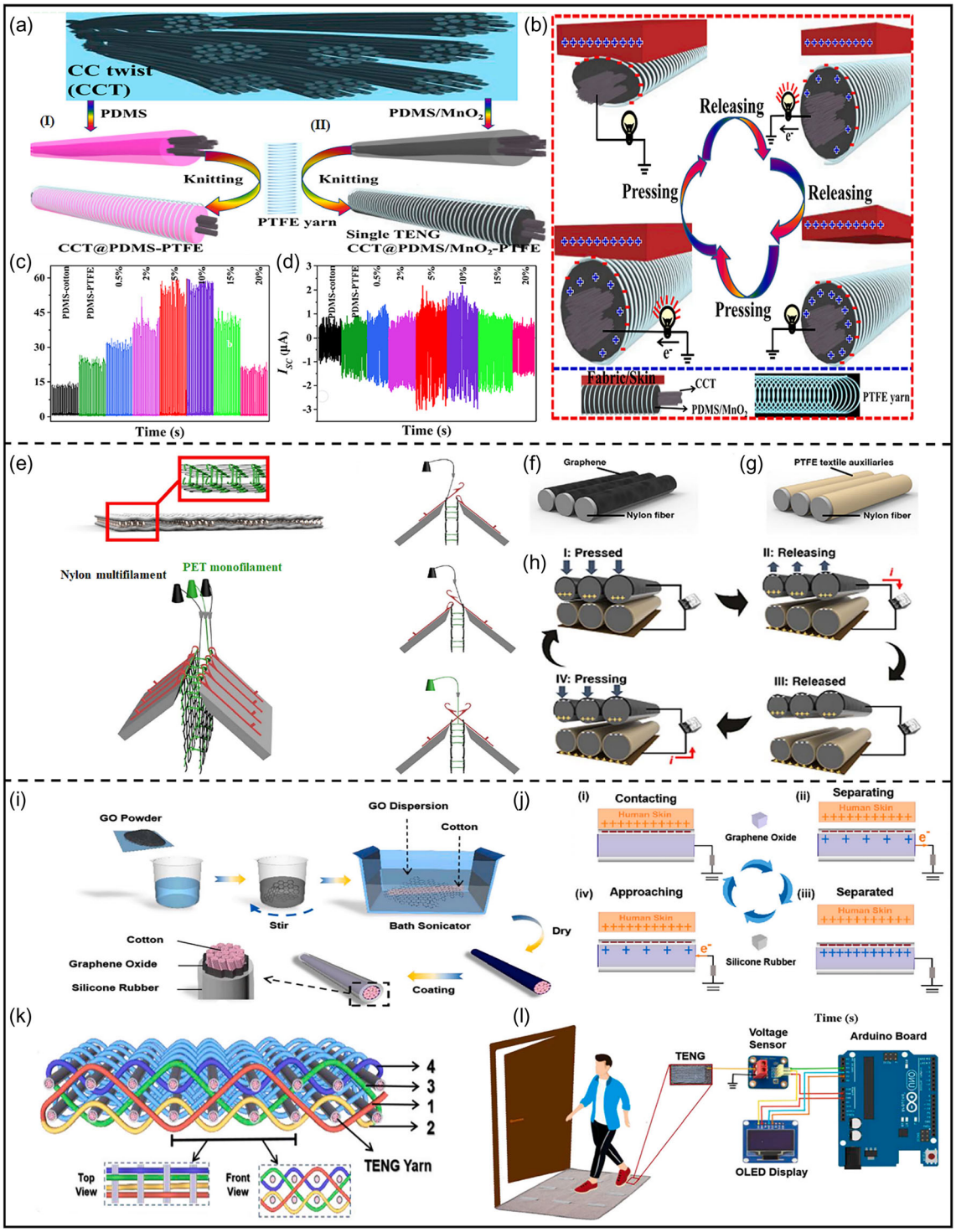

Figure 14. 2D-knitted TENG: a) schematic of the round-tripping knitting process for TENGs: a-I) PTFE yarn closing around pure CCT@PDMS and a-II) CCT@PDMS/MnO_2NW elastic yarns. b) Schematic illustrations of the working mechanism of the T-TENG, c) output voltage, and d) output current of TENGs. Reproduced with permission.[147] Copyright 2021, Elsevier. 3D flat-knitted TENG: e) scheme of the 3D spacer fabric, f) schematically illustration of coating graphene ink onto the upper surface of the upper layer, g) schematically illustration of coating PTFE onto the down layer, and h) the working principle of the 3D-knitted fabric-based TENG. Reproduced with permission.[151] Copyright 2016, Elsevier. 3DAW woven TENG: i) the schematic of preparation process and structure of GO/cotton composite-based TENG yarn, j) schematic diagram of TENG yarn working mechanism in SE mode-based 3D woven fabric, k) the structure schematic of the 3DAW-TENG based on TENG yarn, and l) schematic diagram of carpet signal monitor work. Reproduced with permission.[149] Copyright 2020, Elsevier.

can be said that, despite having structural complexity, 3D woven T-TENG increases the large-scale production capability.

6.2.6. Miscellaneous Fabric-Based T-TENGs

Zhou et al. designed a flexible TENG based on folded carbon paper.[152] The rational geometrical configuration of the structure enabled the optimization of the tensile strain by altering the carbon paper electrode folding angle. The TENG had waterproof and high deformability properties including bending, rolling, and twisting. The fabrication process involved coating carbonaceous powder-based graphite on sandpaper. Following this, electrodes based on folded carbon paper can be obtained through folding method. Later, this newly formed electrode is merged with silicone rubber for fabricating TENG. Chu et al. devised a conformal TENG based on graphene electrode which was plasma treated for galvanizing a nanostructured surface with increased contact area.[153] The electrical output of this conformal TENG is comparable with previously fabricated PDMS–TENG.[111] Moreover, the triboelectric conversion efficiency was further ameliorated upon fabrication of piezoelectric enhanced TENG employing CF as electrode material. Furthermore, a novel conductive biodegradable single-layer TENG was fabricated employing skin friendly silk as frictional substance and CNT as conductive substance.[154] This fabric-based TENG structure was akin to core–shell tube structure, had high power generation capacity as well as impromptu response capability for random human motion. In the structure, the acting CNT electrode forms a microporous structure for the CNT-silk mixing layer which eventually increases the frictional efficiency. The TENG had a spatial arch-shaped configuration which bestows the structure with reliability, adaptability, and less wearing. As a result, output voltage could be generated during activities like flicking human hair, rubbing nylon, or polyester fabric with this CNT-silk mixing film-based glove.

7. Performance and Applications of T-TENGs

The factors that greatly influence the lifetime and performance of T- TENGs are enhanced contact between fibers/yarns, repetitive mechanical pulses, sensitivity of motion, light, humidity, and so on.[44,48,143,155] **Table 4** and **5** present the structure, electrical outputs, carbonaceous nanofillers adaptation technique, washability, stretchability performance, and applications along with special attributes of different fiber-based T-TENG and fabric-based T-TENG respectively. According to Table 4, most fiber-based TENGs were produced by CS and SE modes. Washability performance of these structures is inconspicuous and needs further elaboration. Electrospinning, 3DP, and dip coating are some mentionable methods for combining carbonaceous materials in fiber-based T-TENG structure. Major areas of applications including tactile sensors, strain sensors, patient health monitoring, etc. The output power values of top 3 fiber-based T-TENG were 4120,[156] 3174,[137] and 2500[130] mW m^{-2}. Surprisingly, the TENG devised by wang et al. could sustain 3 million cycles of operation outperforming most fabric-based T-TENG.[134] Similarly, most of the fabric-based T-TENGs were also fabricated by CS and SE modes. Their stability even after 170 000 cycles was testimonial of the structural robustness.[141] It was discernible that there is a paucity of studies regarding washability performance of different T-TENGs structures. The existing literature suggests only 5–6 times washability of fabric-based T-TENGs before the performance starts to degrade.[138,157] The application features of these TENGs were included but not limited to pressure sensors, fitness tracking, smart gloves, etc. The most prospective methods for incorporation of carbonaceous materials in the structure are dip coating and screen printing. Based on Table 5, we can rank fabric TENG produced by Mule et al.,[158] Wu et al.,[39] and Xia et al.[159] as best in terms of output power that were 25 350, 6300, and 4800 mW m^{-2}, respectively. Regarding durability, top 3 fabric-based T-TENGs categorically had 170 000,[141] 90 000,[160] and 75 600[154] cycles of operation withstanding capability.

When evaluating the performance of discussed carbon-based T-TENG, the peak power density of fiber-based TENG and fabric-based TENG devices ranges from 42 μW m^{-2}[161] to 4.12 W m^{-2}[156] and from 70 μW m^{-2}[138] to 25.35 W m^{-2},[158] respectively. It is conspicuous that fabric-based T-TENG always provides better peak power density than fiber-based T-TENG given the fact that the former has less complicated fabrication process which allows them for further surface modification like nanopatterning and plasma treatment. As a result, output performance can further be magnified. Another noticeable thing based on this study is that the upper limit of output performance surpassed the result of previously documented electrical performances of T-TENG which were based on wide range of material choice.[37,65,162] This phenomenon unmasks the appealing impact of carbonaceous material in fabricating TENG devices and justifies their superiority. T-TENG possesses less effective contact area stemming from uneven surface of the textiles produced by interlacement or intermeshing. But application of carbonaceous material like CNT and graphene certainly dispels this problem and results in staggering increase of contact area. Moreover, the evolving 3DP fabric structures can stack multiple layers in the thickness (Z) direction and thus result in exponential growth of contact area compared to 2D fabric TENG and 1D fiber TENG.[65] Although the areal power density of these carbon-based T-TENG seems to be diminutive compared to bulk TENG (500 W m^{-2}),[163] they remain a pervasive source of electricity for different widely used wearable electronics. Based on the available data on power consumption of different on-body electronics (**Figure 15**), it can be concluded that carbon-based T-TENG will not face any difficulty in driving these wearable gadgets.

8. Challenges and Research Gaps

Table 6 highlights the key challenges and research gaps that have been identified from the review of contemporary works presented in the previous sections. These are elaborated in the following subsections.

8.1. Efficiency

The electric nature of T-TENG is quite eccentric and presents a monumental challenge in designing an impeccable circuit. For instance, they generate high voltage sometimes which can reach couple of hundred (620 V[145] for fabric and 276 V[137] for fiber

Table 4. Comparative output performance, mechanical properties, and application of carbon-based fiber T-TENG.

Triboelectric materials	Electrode	Fabrication method	Electrical outputs			Mode	Stretchability/ Durability	Washable	Special attributes	Applications	References
			Voltage	Current	Output power						
Silicone rubber and nylon	Carbon fiber	Winding	42.9 V	0.51 μA	1.12 μW m^{-2}	SE	8000 cycles	Three times	Coaxial fiber structure portrays great storing capacity and inherent flexibility which are fitting for e-textiles	Powering up smart glasses and smart watch	[120]
Silk fibroin and PET	CNT	Coaxial spinneret-based 3D printer	55 V	7 μA	18 mW m^{-2}	CS	15 000 cycles	–	Two diametrically opposite triboelectric materials provide greater output energy, and the spatial 3D structure provides high mechanical durability	e-textiles	[121]
PTFE and CNT	CNT	Dipping and drying	–	11.22 nA,	1 mW m^{-2}	CS	90 000 cycles	–	Can be worn as "power shirt" for rehabilitation and sports training, wireless body temperature monitoring	Wristband for body temperature monitoring,	[118]
Silicone rubber and core electrode	Carbon black/ CNT/silicone rubber composite	Mixing	145 V	16 mAm^{-2}	–	CS	3 million cycles	Washable	Pervasive electric outputs enable this rational TENG to be featured inside 'energy shoes'	Driving fitness tracker, electronic watch, humidity temperature meter	[134]
Silicone rubber	CNT and copper microwire	Dip coating	140 V	0.51 μA	–	CS	70%	–	High flexibility as this TENG is simultaneously stretchable, bendable, and twistable	Powering up self-driven acceleration sensor, digital watch	[133]
PMMA and PDMS	CNT sheets	Wrapping	5 V	240 nA	–	CS	8000 cycles	Washable	Vital monitoring of the finger joint activity	Powering up LCD and LED, velocity direction, and traffic tracking	[122]
$BaTiO_3$/PDMS composite coated on SIS and Ni–Cu fabric coated with nylon 6	Conductive carbon ink	Injecting	76.8 V	7.86 μA	2009 mW m^{-2}	CS	7000 cycles	30 min	Provides uninterrupted power output even when folded or twisted and appealing features remain unchanged up to 250% elongation	Knee protector	[136]
Porous carbon@PEDOT:PSS and PTFE	Gold and porous carbon@PEDOT: PSS	Spin coating	74.3 V	17.9 μA	–	CS	5000 cycles	–	Sublime output performance remains unchanged up to 100% strain	Powering up flexible detector integrated with textile for measuring blood oxygen flow	[128]
Silk and CNT-silk solution	CNT-silk fibroin layer	Electrospray coating	276 V	9.20 μA	3174 mW m^{-2}	SE/ LS	–	Not washable	The tensile strength and softness of the TENG structure conform to the wearing requirements of textile	Powering up humidity thermometer	[137]
Carbon cloth with bimetallic copper–nickel nanowrinkles and PTFE	Copper–nickel bimetallic hydroxide	Hydrothermal method	328 V	36.15 μA	1323 mW m^{-2}	CS/ LS	5000 cycles	–	Functional in both contact-separation and LS mode and sometime in their compound principle. Spherical shaped nanostructure produces highest electrical performance due to astounding contact area	Powering up LED, electrical calculator, self-driven touch sensor, human motion posture sensor	[131]

Table 4. Continued.

Triboelectric materials	Electrode	Fabrication method	Electrical outputs			Mode	Stretchability/ Durability	Washable	Special attributes	Applications	References
			Voltage	Current	Output power						
Polycation-modified carbon dots incorporated with nanocomposite polymer electrolytes and PDMS	Silver plated nylon yarn	Core–sheath inserting	23.8 V	0.9 μA	265.8 μW m^{-2}	SE	30 000 cycles	10 times	Carbon dot materials used in the structure render incredible ionic conductivity, charge mobility, and dispersibility which are conducive to higher electrical output	Powering up smart glove, electronic calculator, possession of voice recognition features	[125]
Latex–CNT composite–PDMS dip-coated elastomer yarn and bare elastomer yarn	CNT-based composite solution	Dip coating	43.7 V	0.19 μA	11.89 μW cm^{-2}	FS	3000 cycles	–	The TENG has astounding water resistance properties along with resistance to folding, twisting, and stretching	Powering up different wearable energy harvesters	[123]
CNTs–parafilm and CNT–PDMS	Silver	Stacking	28 V	–	–	SE	1500 cycles	–	Precisely detect both stress and strain as well as the texture, shape, type, mass, and position of the object	Tactile sensors, patient health monitoring	[124]
Polyethersulfone and cellulose	Carbon black	Electrospinning	115 V	9 μA	0.13 W m^{-2}	CS	6000 cycles	–	Electrospinning nanofibrous membrane-based three-layer WTENG which boosts the voltage and current 2.56 times and 3.07 times than single layered TENG	Energy harvesting from commercial kneepad, driving small electronics	[197]
Stretchable Ecoflex	MWCNT–polyaniline derivatives and varnished wire	Dip coating	0.2 V	12.5 nA	4.2×10^{-5} W m^{-2}	CS	250%	–	The TENG is extremely sensitive to surrounding atmosphere and environmental conditions. Thus, it can be used in uncloaking environmental atmosphere	Energy harvesting	[161]
PVDF-TrFE and nylon/PU	Ag and CNT	CVD	240 mV	8 nA	–	CS	10 000 cycles	–	The conspicuous wrinkle formation was induced by the difference in poison's ratio between coated nylon and CNT-incorporated layer	Energy harvesting and detecting human motion	[127]
Poly vinylidene fluoride–hexafluoropropylene and nylon	rGO	Electrospinning	300 V	7 μA	500 mW m^{-2}	SE	1600 cycles	–	Crumpled structure of graphene attributes for higher electrical conductivity of TENG	Energy harvesting for wearable textile	[129]
Graphene and PDMS	Graphene	Spin coating	83 V	25.78 μA	2500 mW m^{-2}	CS	120%	–	The output performance surged with the increment of crumpled degree	Self-powered strain sensor	[130]
Graphene and PDMS	Graphene	CVD	22 V	0.9 μA	–	CS	–	–	Sustainable fabrication method of graphene into TENG	Wearable device	[132]
PDMS	CNTs mixed with Ag NWs	Dip coating	22 V	0.2 μA	21.5 μW m^{-1}	SE	140%	Washable	Can record number of footsteps, hand gestures, bending of fingers	Biomechanical monitoring	[198]
Silk and PDMS	Graphite	Screen printing	666 V	175 μA	4120 mW m^{-2}	SE	–	–	Endowed with crucial selective absorption nature	Wearable multifunctional sensor	[156]
PDMS with PTFE and PDMS with graphene	Graphene	3DP	–	–	–	SE	350%	Washable	Triboelectric signal is enhanced 1.8 times by combining PTFE with PDMS	Tactile sensor	[126]

Table 5. Comparative output performance, mechanical properties, and applications of carbon-based fabric T-TENG.

Triboelectric materials	Electrode	Fabrication method of carbonaceous materials in T-TENG	Electrical outputs			Modes	Stretchability/ Durability	Washable	Special attributes	Applications	References
			Voltage	Current	Output power						
PU–PI and PDMS–Al	CNT	CVD	15 V	130 nA	1800 μW m^{-2}	CS/LS	4000 cycles	–	Unique structure that discards the prerequisite of air gaps, provides necessary current for powering external pressure sensor	Powering up LED, electronic watch, wearable sensors for monitoring daily activities	[15]
Silk and skin	CNT	Screen printing	7 V	160 nA	–	SE	10 000 cycles	15 h	The fabricated E-textile features improved sensitivity, rapid response, uninterrupted cycle performance, and conforms breathability of textile	Self-driven gesture sensors to access computer software, controlling bulbs, wirelessly controlling microwave ovens	[142]
PTFE and cotton	Conductive carbon wires	Shuttle weaving	118 V	1.5 μA	–	CS/FS	15 000 cycles	–	Weaving this TENG and SC in a unified structure ensures robustness without compromising mechanical flexibility of textile	Powering up electronic watches and other sensors	[52]
Graphene and polyester	Ag NWs	Blade coating	14.5 V	2 μA	70 μW m^{-2}	LS	34%	Six times	TENG remains electrically stable even under extreme folding or curling	Smart glove that can generate electricity from the movement of the fingers	[138]
CNT–PDMS-coated Ag textile and nylon cloth	Copper	Brush coating	51.2 V	3.0 μA	99.8 mW m^{-2}	SE/CS	10 000 cycles	Washable	Novel brush model enhanced the biological compatibility, implantability, and durability of T-TENG	Powering up LED, precise identification and collection of energy	[140]
PTFE–nylon and nylon	Graphene ink	Computerized flat knitting-based 3D weft knitting	3 V	0.3 μA	16 μW m^{-2}	CS	–	–	3D weft knitting spacer technology enables the intelligent designing of pressure sensitive small pixelated TENG arrays which can accurately measure each step	Powering up LED, applied as pressure sensor during walking	[151]
CNT and polyetherimide grafted velvet fabric–PTFE film	Conductive fabric attached with copper wires	Chemical grafting	119 V	12.6 μA	3.2 W m^{-2}	CS	1000 cycles	24 h	Creating carbonaceous hierarchical structure on the surface of the fabric for better triboelectric output without compromising the inherent mechanical properties (dimensional stability, abrasion resistance) of fabric	Powering source for digital watch, pedometer, calculator along with self-powered pressure and tactile sensing	[143]
Silicone rubber and skin	Folded carbon paper	Mold casting	330 V	18.6 μA	32.2 mW m^{-2}	SE	–	Washable	The spatial design of TENG allows carbon electrodes to fold into different angles and remain highly sensitive to mechanical motions (twisting, stretching, rolling, and folding)	Powering up LEDs, electronic watch	[152]
PDMS coated on textile substrate and skin	Carbonized cotton fabric coated with rGO	Dip coating	17.8 V	83 nA	0.8 μW cm^{-1}	SE	2000 cycles	–	Understanding of Morse-code	Powering up LEDs, utilized as self-powering information delivery medium	[146]
Silicone rubber and skin	MWCNT-coated self-healable electrode	Embedding	95 V	1.5 μA	750 mW m^{-2}	SE	400%	–	This environment friendly TENG was also electrically and mechanically self-healable	Powering up soft devices, LEDs	[199]

Table 5. Continued.

Triboelectric materials	Electrode	Fabrication method of carbonaceous materials in T-TENG	Electrical outputs			Modes	Stretchability/ Durability	Washable	Special attributes	Applications	References
			Voltage	Current	Output power						
CNT-based functional elastomer layer and nitrile–butadiene rubber composite	Conductive fabric	Blade coating	620 V	51 μA	1.6 mW cm^{-2}	CS	5000 cycles	24 h	Outstanding deformability, flexibility, and robustness pave the way for TENG to be firmly integrated with textile	Powering up LED, quartz watch, wearable glove to interact with machine interface	[145]
CCT@PDMS–MnO_2NW and PTFE	Twisted carbon yarn	Dipping and drying	380 V	–	–	CS	3000 cycles	Washable	Introduction of a novel round-tripping-knitting strategy for the fabrication of a yarn-based TENG with high degree of freedom.	Powering up LED and precise pressure sensing	[147]
Nylon cloth and PDMS	BC–CNT–PPy macrofiber and silver	Physical doping	170 V	0.8 μA	54.14 mW m^{-2}	CS/SE	100 cycles	washable	Degradability within 108 h corroborates superior environmental friendliness of this fabric-based TENG	Driving humidity-temperature meter, calculator, electronic watch, and monitoring human motions	[139]
PWA (PEO/WPU/alliin) and skin	PEI/MWCNT/phytic acid	Core–sheath inserting	137 V	2.1 μA	2.25 mW m^{-2}	SE	500 cycles	–	This yarn TENG pushes forward the research on interaction of human-machine and artificial intelligence	Lighting up LED, driving digital alarm clock and various strain sensors, guiding the rehabilitation of patients	[135]
Silver (Ag) NP-coated graphitic carbon nitride (g-C_3N_4) (AgCN)–nylon bilayer and Teflon	Conductive carbon cloth and Al	Plain woven	200 V	1.1 μA	31 mW m^{-2}	CS	1000 cycles	–	Maintains higher efficiency of power conservation at an elevated temperature of 65 °C which dictates its superior thermal stability	Sensors for accessing remote locations and detecting human motions	[102]
PET-coated 3D textile structure and PDMS-coated textile structure	CNT and Ag	Penetrated structure	500 V	20 μA	153.8 mW m^{-2}	CS	3000 cycles	–	Highly flexible design as no conspicuous damage in structure was observed for 0° to 180° angle bending	Energy harvesting	[144]
PDMS and PET	Graphene	Layer stacking	47.1 V	7 μA	144 mW m^{-2}	SE	–	–	Conformal skin attachable TENG with thickness of just 2.4 μm	Assistive device for communication	[111]
Cotton fabric and PDMS	CNT	Weft knitting	200 V	0.6 μA	37.5 mW m^{-2}	SE	170 000 cycles	–	26.6% wireless transmission efficacy	Smart patch for healthcare	[141]
PVDF and silk	CF	Electrospinning nanofibers	500 V	12 μA	3100 mW m^{-2}	CS	10 000 cycles	–	Wearable fall alert detection	Harvesting high power energy	[153]
CNT and PTFE	CNT	Drop drying	100 V	2 μA	121 mW m^{-2}	SE	10 000	5 times	Synced with a supercapacitor which provides a stable performance	Energy harvesting, operating calculator	[157]
Silk and PET	CNT	Slide coating and drop coating	262 V	8.73 μA	2859 mW m^{-2}	SE	75 600 cycles	–	Lower cost, production friendly structure with the added features of lightweight, softness, and minute sensibility	Powering up LED, biomechanical sensors, and motion sensors	[154]
PDMS and skin	Graphene and Cu	Spin coating and electrodeposition	60 V	–	91.9 mW m^{-2}	SE	10 000 cycles	–	Realizing a Cu/graphene heterostructure-based TENG for avoiding copper oxidation	Wearable devices	[110]

Table 5. Continued.

Triboelectric materials	Electrode	Fabrication method of carbonaceous materials in T-TENG	Electrical outputs			Modes	Stretchability/ Durability	Washable	Special attributes	Applications	References
			Voltage	Current	Output power						
PTFE and cotton	Graphene and Al	Transferring	68 V	14.4 μA	–	CS	1000 cycles	–	Fabrication of graphene-based personal protective equipment against biological and chemical threats	Powering up LEDs	[200]
Aligned graphene sheet embedded PDMS and Cu	Cu	Spin coating	530 V	21 μA	4800 mW m^{-2}	CS	Several days	–	Higher voltage of breakdown and less dielectric loss	Height sensor	[159]
GO and skin	Al	Stacking	1100 V	55 μA	3130 mW m^{-2}	SE	–	–	Possess excellent sensitivity	Self-powered sensors, wearable electronics	[201]
rGO–PI (Kapton) and Al	Al	Spin coating	190 V	–	6300 mW m^{-2}	CS/LS	–	–	Utilizing rGO as electron trapping site enhanced the output by 30 times	Energy harvesting	[39]
Graphene and PTFE	Graphene	Dip coating	100 V	5 μA	–	SE	20 000 cycles	–	Very first graphene-based T-TENG fabrication through layer by layer deposition method	e-textile	[202]
PVDF and nylon	Graphene and gold	Doctor blading	80 V	–	286 mW m^{-2}	CS	–	–	Graphene attributes for 26 times increase in power density	Energy harvesting	[203]
MWCNT embedded into nylon and PDMS	Al	Spin coating	270 V	15 μA	25.35 W m^{-2}	CS	12 000 cycles	Washable	Electrical output remained stable at wide range of humidity of 30–80%	Touch sensing, energy harvesting during running, and walking	[158]
CNT–PDMS and PDMS	CNT and Au–Ti	Sandpaper templating	17 V	0.18 μA	–	CS	Up to thousands of cycles	–	Sandpaper-based less complicated fabrication method	Wearable pressure sensor	[204]
Silicone Ecoflex and skin	CNT	Ink-jet printing	–	–	33.5 mW m^{-2}	SE	30%	–	Fabrication of a super stretchable CNT electrode through lateral combing process which maximizes the percolation probability	Energy harvesting	[184]
CNT–PDMS and Al	Al and conductive textile	Blade coating	21.5 V	–	–	CS	90 000 cycles	–	CNT doping magnified the output voltage 7 times along with higher sensitivity and fast response	Tactile sensor for monitoring human conditions	[160]
Silicone rubber and skin	GO–cotton	Dip coating	30.8 V	1.1 μA	225 mW m^{-2}	CS	–	–	Better electrical attributes than 3D double layer plain structure and 2D plain structure	Powering voltage sensors	[149]
Pure PDMS and porous CNT–PDMS	CNT–PDMS double spiral layer	Magnetic stirring and solidification	–	–	–	FS	–	–	Mimics fast adaptable real skin. Weight fraction of CNT modulates the sensitivity of skin	Powering pressure detector sensor	[205]
CNT and polyglycerol sebacate	CNT	Direct ink writing	170 V	–	185.2 μW m^{-2}	SE	6000 cycles	–	3DP-based hierarchical porous structure outperforms traditional fabrication methods and simultaneously utilizes sustainable materials	Self-powered lightweight shoe	[206]
MWCNT-doped PVDF and nylon	Aluminum	Plain woven	7 V	700 nA	850 μW m^{-2}	FS	–	–	PVDF was created by electrospinning process which in combination with doped MWCNT significantly enhanced surface area and hence triboelectric charge density	Integration with floor mats, cloth, shoes for Energy harvesting	[207]

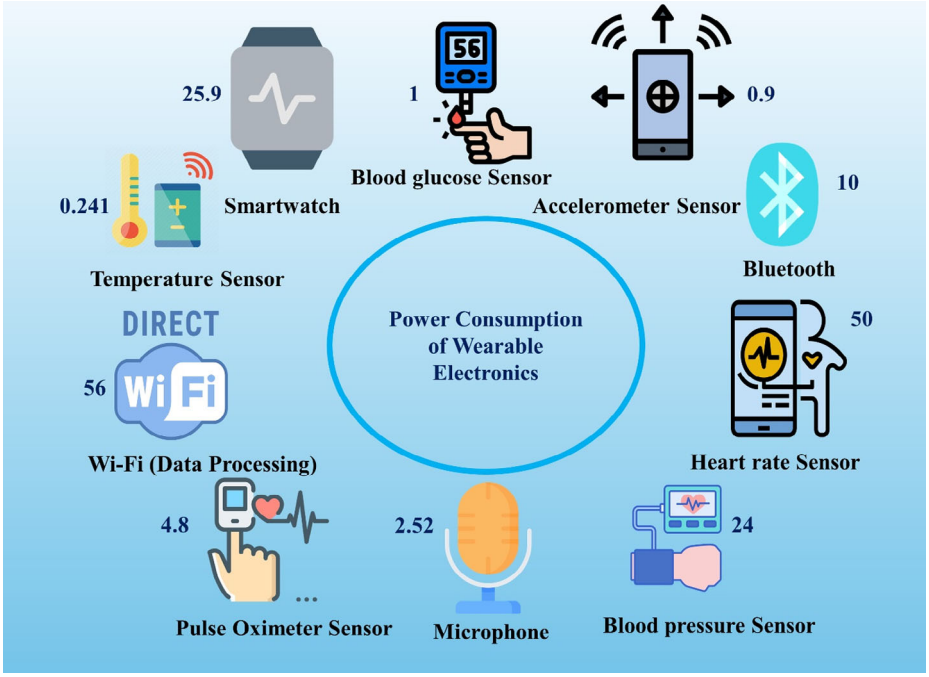

Figure 15. Power consumption of wearable electronics (numerical values are in mW).[181,185,186]

Table 6. Key challenges and research gaps regarding the future of T-TENGs.

Challenges	Research gaps
Increasing efficiency	Increasing the surface area attributed to uneven surface of textile, prevention of destabilization due to higher internal resistance of T-TENG
Ensuring wearer comfort	Chemically treating fabric surface without compromising breathability and aesthetics, guaranteeing enduring tactile comfort of the clothing
Improved washability	Testing against international washing standards (AATCC 135, ISO 6330) that are widely adopted in the textile industry, introduction of novel fabrication process conforming washability
Higher durability	Reduction of the extensive consequences of frictional contact on lifespan and performance degradation of T-TENG
Scalability	Developing a real clothing that can harvest energy from the entire garment, adopting fully fashion knitwear instead of traditional roll-to-roll knitting process, redefining the sizing technology to increase the weavability
Safety	Preparation of safety guidelines, assessment the risk factor of electrostatic shock on human body, devising T-TENGs that do not bring any adverse impact on human skin
Better stability	Working under extreme environments like higher temperature, humidity, or pressure
Higher mechanical resistance	Implementation of nuanced mechanical designs, incorporation of self-healing ability

based on the current study). But their output current associated with it is quite the opposite. It mainly ponders around μA unit and can sometimes even drop into nA (83 nA[146] for fabric and 8 nA[127] for fiber based on the current study). Because of the higher internal resistance of these T-TENGs, only a small amount of voltage can be utilized based on the load resistance theorem as electrical outputs tend to be smaller than output voltage.[48] Power conditioning units (buffer, rectifier) play a critical role in preventing destabilization and can increase the energy conversion efficiency of the device.[164] Prospectively, structural design is crucial for alleviating lower efficiency. FS mode-based T-TENGs are most effective for attaining higher power conversion efficiency (85%).[165] In this method, energy can be harvested through independently moving objects. It should be noted that there is still a scarcity of research on augmenting the power conversion efficiency of carbon-based T-TENG. Another remedy for lower output power can be the introduction of many small-sized TENGs together. Recently, textile-based SCs are being effectively integrated with T-TENG for stabilizing the output power.[15,42,52,121,134] So it is obvious from these studies that power management circuits are required for achieving better efficiency of T-TENG.[166] A pragmatic approach for indexing the performance of T-TENG should be based on measuring the time required to fully charge a capacitor. Any leakage of current during energy storage will result in lower efficiency. Textiles also have complicated configurations of hierarchical structure from

fiber to fabric. In the future, researchers should establish a simulation model that can predict complex hierarchical structure of textile and accordingly integrate carbonaceous nanofiller for achieving better output efficiency of T-TENG.

8.2. Wearer Comfort

Breathability of textile is vital factor for ensuring wearer's comfort.[167] It involves permeability of water, air, moisture, light, and heat that have impact on regulating the balance of humidity and temperature in human body. Different types of surface patterning or treatment can reduce the breathability of the textile by reducing space between the fibers. Also, carbon-based materials further impair the breathability performance. While integrating carbon-based TENG with textiles, it is important to ensure that the inherent properties of textile are not altered by any means of fabrication. Textile structures translate their natural flexibility into T-TENG, which enables them to curl, fold, twist, or mold in both fabric and fiber form.[133,168] Sustaining the natural flexibility of fabrics without compromising the triboelectric properties is still an ongoing effort by researchers. The major impediment here is that the application of different coatings will certainly change the surface characteristics of fabrics. Future research on carbon-based wearable T-TENG should look into how natural textile features and triboelectric performance can be made more mutually inclusive.[167] Tactile comfort, which is another perception of wearability, includes prickle sensation, cold stimulation, and fabric weight.[37] As T-TENG will scavenge mechanical motion during active performances like running, walking, or sprinting, maintaining comfort to wearer during these activities is of paramount importance.

8.3. Washability

Washability is another vital issue of T-TENGs because a normal cloth needs to withstand detergents, drying, washing, and ironing. It is obvious from Table 4 and 5 that most literature still does not consider washability performance seriously. This is a big loophole that needs to be addressed properly. A wearable energy harvesting device should be designed as complete garment rather than just integrating textile-based TENG into a portion of existing clothing so that the actual clothing can be washed according to the international standards like ISO (International Organization for Standardization) and AATCC (American Association of Textile Chemists and Colorists). Unfortunately, there is no literature that has described the impact of industrial scale washing on the bonding, fixing, and adhesion properties among different constituents of T-TENG. So, washability prospect of T-TENG devices remains an unexplored field and can be of great interest for future researchers. Nevertheless, some approaches have been put forward to deal with the washability issue. In a bid to create a favorable washing condition, T-TENGs can be encapsulated with waterproofing materials. However, this leads to weaving difficulty, lower breathability, and increased fabric weight. Nesting triboelectric and electrode constituents together in the textile structure by plating rather than traditional simple attachment represents a good prospect for washability.[148] Plating is a novel knitting technique that allows two different threads to be separately knitted at the technical face and technical back of the knitted fabric. Similarly, self-stitched double cloth-based woven fabric structure can also have a bright prospect regarding washability performance. Besides, a single-step surface coating by conductive polymers via simultaneous electrospinning and electrospray can also exhibit great washability performance.[169]

8.4. Durability

Durability aspects include materials pilling and abrasion, dimensional stability to length and width, spirality (for knitted fabric), untwisting of yarns, drying, and wrinkling capability.[48] Among them, abrasion test should be performed rigorously to quantify the lifetime of T-TENG device because the principle of TENG rests on frictional contact between two different triboelectric materials. FS mode experiences less friction compared to other methods and is much more suited for avoiding abrasion. However, most literature overlooks the durability prospects in line with the seamless conductivity translated by carbonaceous materials. Prospectively, carbonaceous materials like CNT, graphene, CF, etc. possess a unique nature of fabricating lightweight T-TENG. Making the T-TENG more lightweight without compromising its conductivity is a matter of interest in ongoing research.[170]

8.5. Scalability

A major challenge is the large-scale fabrication of carbon-based T-TENG. For instance, large-scale fabrication of fiber-based TENG is extremely difficult due to the progressive decline of conductivity with the increase in length.[171] Carbonaceous materials prevent this declining tendency only to some extent. Second, sometimes fabricated warp and weft yarn in a weaving procedure cannot withstand the higher tensile strength requirement (50 MPa) during the shedding and picking mechanism. Carbon material-coated T-TENG also cannot be treated with conventional sizing processes. It turns out that the structure then becomes susceptible to delamination and crack propagation.[172] Moreover, T-TENGs are generally produced in roll form which can later be cut in half with each constituent having half of the original output. Later, pieces can be sewn together to get the full output. But unfortunately, the electrodes have to be manually reconfigured which is a time-consuming and error-prone process.[173] Furthermore, sensing accuracy undeniably will be crucial element for these T-TENGs commercialization which is hardly achieved by existing carbonaceous-incorporated T-TENGs in the market. Additionally, due to the weak interfacial bonding between rigid carbon material-based electronics and soft textile materials, maintaining conformability during mass production will be a big challenge for future research. Finally, utilizing carbonaceous T-TENG during stationary positions should also be highlighted as the prerequisite of continuous human movements limits the scalability of these T-TENGs.[37]

8.6. Safety

Besides wearability, washability, and durability, safety is a major concern for the industrial application of carbon nanofiller-based

T-TENGs.[174] The concept of safety revolves around several aspects including thorough assessment of electrical components' impact on physiology of human body and environmental ecology. They are also susceptible to electrolyte leakage, ohmic heating, and stress concentration leading to breakage. Concerns are also around regarding electrostatic shock generation on human body as many operational modes are based on friction. These devices are also not protected against perspiration which further jeopardizes the device's safety. These NGs certainly remain exposed to human skin. So, the selected materials must be nontoxic and highly biocompatible. The evaluation standard and user safety guidelines of these structures are not properly established either. For instance, different T-TENGs generally have incongruous test conditions (contact area, material modification, working environment, applied load, etc.) which yield ambiguous and often misleading results. There is also limited research on anti-flammability, water resistance, and thermal insulation behavior which should also be discussed in future research.

8.7. Working Stability

The spatial nanotopographic structures imparted by carbonaceous nanofillers on textile structures can be impaired by complex and intense chemical treatment or mechanical load. The electrical outputs of T-TENG are impeded by external environments (temperature, pressure, water, humidity, radiation, absorption, and gas). Higher temperature subdues the performance of T-TENGs.[175] High humidity and contaminants can degrade the charge transfer process between triboelectric materials.[42,176] The issue of working stability cannot be condoned because the idea of using TENGs multiple times is getting popular. So, more research should be carried out to exploit the role of carbonaceous material in augmenting high-humidity tolerance, high pressure, and temperature resistance in T-TENG structures.

8.8. Mechanical Resistance

Mechanical resistance is one of the vulnerabilities of T-TENG because the mechanism is entirely dependent on the frictional contact between two triboelectric materials which inevitably degrades the mechanical resistance. As a result, the output performance and stability of electricity are compromised. Researchers are continuously exploring new ways to circumvent these situations including designing mechanically durable devices by lubrication.[81] By introducing right thickness lubricant liquid film, frictional coefficient between the triboelectric materials can be significantly reduced. Subsequently, the resilience of self-healing polymers substantially improves the mechanical resistance of TENG. Due to the presence of special bonds (reversible covalent mode, dynamic covalent bond), self-healing polymers effectively regroup at the broken site leading to the restoration of chemical bonds. So, the incorporation of carbon-based composite materials involving self-healing polymer in T-TENG can augment the mechanical resistance as textile can repair back itself. Besides, devising TENG based on nuanced mechanical design guidelines involving mechanical elements like gear train, cam system, and spring for energy transmission also excels the mechanical resistance.

9. Conclusion

Clothing is one of the basic needs of human beings. About 100 billion garments are produced each year.[177] With the rise of IoTs, it is predicted that global usage of smart wearable devices will reach US$ 23.82 billion by late 2031.[178] Integration of electronics with textiles at the industrial level is progressing rapidly, as this can lead to an on-body platform for seamless computing while retaining astounding features of textiles, including superior comfort, flexibility, washability, excellent mechanical strength, excellent air permeability, lightweight, and foldability. T-TENG can play a pivotal role in the field of smart wearables. T-TENG as a power source imparts energy autonomy to wearable electronics by eliminating the battery source. The performance of these T-TENGs was greatly improved by employing carbonaceous nanofiller as electrode or triboelectric materials. Among the carbonaceous nanofillers, 1D CNT and 2D graphene and their derivatives have the most stunning impact on T-TENGs.

In a bid to provide design guidance for these emerging materials; basic operation modes, versatile textile structures for TENG, different fabrication methods pertinent to carbonaceous materials incorporation, and commonly used low-dimensional carbonaceous nanofillers and their performance on these T-TENGs were discussed. T-TENGs have great potential in self-powered systems, wearable sensors, identity recognition, health monitoring, etc. Among different textile structures, weaving is most popular for symmetrical contact surfaces due to its higher dimensional stability, durability, higher strength and surface area, and lower thickness which are suitable for CS, FS, and LS mode-based T-TENGs.[36] However, knitting is conducive for asymmetrical contact surfaces due to the advantageous nature of elasticity and deformation easiness, which are opted for SE and CS mode-based T-TENGs. Consequently, knitted structures are susceptible to pilling, snagging, and shrinkage and are rarely used during FS or LS modes. Nonwoven and braiding-based T-TENGs are rarely developed due to their inherent shortcomings in the structure. Fabric-based TENGs possess higher output efficiency but poor wearability. Contrary to that, fiber-based TENGs have higher deformability but poor compatibility with prevailing manufacturing processes. Inconsistent contact electrification can be alleviated by nanopatterning with carbonaceous nanofillers, which can be further supplemented by 3D fabric structures. Simultaneously, carbonaceous materials regulate surface roughness and energy, increase surface area and porosity, control geometric morphology, and augment polarity which are beneficial for attaining higher energy conversion efficiency of T-TENGs. Finally, described T-TENGs were ranked based on their performance and future challenges were also transcribed. This article successfully unearthed the synergy between carbon materials, textiles, and TENGs. Researchers from diverse fields including materials, textiles, and electronics will benefit from this review. Smart textile manufacturers can use the findings for the proper selection of triboelectric, electrode, and carbonaceous materials, along with fabrication methods during manufacturing and commercialization of their T-TENGs.

Conflict of Interest

The authors declare no conflict of interest.

Author Contributions

Abdullah Sayam: Conceptualization (equal); conceptualization (lead); writing—original draft (lead); review; editing. **Md. Mahfuzur Rahman:** Conceptualization (equal); writing—original draft (second lead); review; editing. **Abu Sadat Muhammad Sayem:** Conceptualization (equal); conceptualization (lead); review; editing. **A. T. M. Faiz Ahmed:** Conceptualization (equal); review and editing. **Shah Alimuzzaman:** Conceptualization (equal); review and editing.

Keywords

carbonaceous materials, energy harvesting, sustainability, textiles, triboelectric nanogenerators

Received: April 25, 2024
Revised: July 6, 2024
Published online:

[1] H. M. Reeve, A. M. Mescher, A. F. Emery, in *Proc. 2001 ASME Int. Mechanical Engineering Congress and Exposition*, New York, NY **2001**.
[2] Z. L. Wang, *Nano Energy* **2019**, *58*, 669.
[3] T. Q. Trung, N. Lee, *Adv. Mater.* **2016**, *28*, 4338.
[4] C. Sun, J. Liu, Y. Gong, D. P. Wilkinson, J. Zhang, *Nano Energy* **2017**, *33*, 363.
[5] J. Fu, Z. P. Cano, M. G. Park, A. Yu, M. Fowler, Z. Chen, *Adv. Mater.* **2017**, *29*, 1604685.
[6] D. H. P. Kang, M. Chen, O. A. Ogunseitan, *Environ. Sci. Technol.* **2013**, *47*, 5495.
[7] H. Askari, N. Xu, B. H. G. Barbosa, Y. Huang, L. Chen, A. Khajepour, H. Chen, Z. L. Wang, *Mater. Today* **2022**, *52*, 188.
[8] Z. Zhao, Y. Dai, S. X. Dou, J. Liang, *Mater. Today Energy* **2021**, *20*, 100690.
[9] J. T. Nguyen, W. Cheng, *Small Struct.* **2022**, *3*, 2200034.
[10] X. Chen, Y. Liu, Y. Sun, T. Zhao, C. Zhao, T. A. Khattab, E. G. Lim, X. Sun, Z. Wen, *Nano Energy* **2022**, *98*, 107236.
[11] C. Chen, H. Guo, L. Chen, Y. C. Wang, X. Pu, W. Yu, F. Wang, Z. Du, Z. L. Wang, *ACS Nano* **2020**, *14*, 4585.
[12] Y. Zi, H. Guo, Z. Wen, M. H. Yeh, C. Hu, Z. L. Wang, *ACS Nano* **2016**, *10*, 4797.
[13] C. Chen, Z. Wen, J. Shi, X. Jian, P. Li, J. T. Yeow, X. Sun, *Nat. Commun.* **2020**, *11*, 4143.
[14] G. Chen, J. Wang, G. Xu, J. Fu, A. B. Gani, J. Dai, D. Guan, Y. Tu, C. Li, Y. Zi, *EcoMat* **2023**, *5*, 12410.
[15] S. Jung, J. Lee, T. Hyeon, M. Lee, D. H. Kim, *Adv. Mater.* **2014**, *26*, 6329.
[16] R. Walden, I. Aazem, A. Babu, S. C. Pillai, *Chem. Eng. J.* **2023**, *451*, 138741.
[17] S. Bairagi, G. Khandelwal, X. Karagiorgis, S. Gokhool, C. Kumar, G. Min, D. M. Mulvihill, *ACS Appl. Mater. Interfaces* **2022**, *14*, 44591.
[18] I. Domingos, A. I. S. Neves, M. F. Craciun, H. Alves, *Front. Phys.* **2021**, *9*, 742563.
[19] J. H. Choi, Y. Ra, S. Cho, M. La, S. J. Park, D. Choi, *Compos. Sci. Technol.* **2021**, *207*, 108680.
[20] X. Cui, H. Wu, R. Wang, *J. Mater. Chem. A* **2022**, *10*, 15881.
[21] J. Lama, A. Yau, G. Chen, A. Sivakumar, X. Zhao, J. Chen, *J. Mater. Chem. A* **2021**, *9*, 19149.
[22] M. A. Gabris, J. Ping, *Nano Energy* **2021**, *90*, 106494.
[23] K. Cheng, S. Wallaert, H. Ardebili, A. Karim, *Carbon* **2022**, *194*, 81.
[24] F. R. Fan, Z. Q. Tian, Z. L. Wang, *Nano Energy* **2012**, *1*, 328.
[25] Q. Lu, M. Sun, B. Huang, Z. L. Wang, *Adv. Energy Sustainability Res* **2021**, *2*, 2000087.
[26] S. Kwon, Y. H. Hwang, M. Nam, H. Chae, H. S. Lee, Y. Jeon, S. Lee, C. Y. Kim, S. Choi, E. G. Jeong, K. C. Choi, *Adv. Mater.* **2020**, *32*, 1903488.
[27] C. Wu, A. C. Wang, W. Ding, H. Guo, Z. L. Wang, *Adv. Energy Mater.* **2019**, *9*, 1802906.
[28] S. I. Tushar, A. Sayam, M. M. Uddin, T. M. Dip, H. R. Anik, M. R. A. Arin, S. Sharma, *J. Mater. Chem. A* **2023**, *11*, 19244.
[29] K. Y. Song, S. W. Kim, D. C. Nguyen, J. Y. Park, T. T. Luu, D. Choi, J. M. Baik, S. An, *EcoMat* **2023**, *5*, 12357.
[30] R. Zhang, H. Olin, *EcoMat* **2020**, *2*, 12062.
[31] J. Zhou, H. Wang, C. Du, D. Zhang, H. Lin, Y. Chen, J. Xiong, *Adv. Energy Sustainability Res.* **2022**, *3*, 2100161.
[32] Z. L. Wang, *Mater. Today* **2017**, *20*, 74.
[33] T. M. Dip, M. R. A. Arin, H. R. Anik, M. M. Uddin, S. I. Tushar, A. Sayam, S. Sharma, *Adv. Mater. Technol.* **2023**, *8*, 2300802.
[34] Q. Miao, C. Liu, N. Zhang, K. Lu, H. Gu, J. Jiao, J. Zhang, Z. Wang, X. Zhou, *ACS Appl. Electron. Mater.* **2020**, *2*, 3072.
[35] Y. Chen, Y. Ling, R. Yin, *Sensors* **2022**, *22*, 9716.
[36] S. Kim, M. K. Gupta, K. Y. Lee, A. Sohn, T. Y. Kim, K. S. Shin, D. Kim, S. K. Kim, K. H. Lee, H. J. Shin, D. W. Kim, *Adv. Mater.* **2014**, *26*, 3918.
[37] K. Dong, X. Peng, Z. L. Wang, *Adv. Mater.* **2020**, *32*, 1902549.
[38] C. Wu, T. W. Kim, H. Y. Choi, *Nano Energy* **2017**, *32*, 542.
[39] R. Zhou, Y. Zhao, R. Zhou, T. Zhang, P. Cullen, Y. Zheng, L. Dai, K. Ostrikov, *Carbon Energy* **2023**, *5*, 260.
[40] V. Strauss, A. Roth, M. Sekita, D. M. Guldi, *Chem* **2016**, *1*, 531.
[41] K. Dong, Y. C. Wang, J. Deng, Y. Dai, S. L. Zhang, H. Zou, B. Gu, B. Sun, Z. L. Wang, *ACS Nano* **2017**, *11*, 9490.
[42] J. Zhu, M. Zhu, Q. Shi, F. Wen, L. Liu, B. Dong, A. Haroun, Y. Yang, P. Vachon, X. Guo, T. He, *EcoMat* **2020**, *2*, 12058.
[43] G. Chen, Y. Li, M. Bick, J. Chen, *Chem. Rev.* **2020**, *120*, 3668.
[44] B. Zhang, T. Ren, H. Li, B. Chen, Y. Mao, *Adv. Energy Sustainability Res.* **2024**, *5*, 2300245.
[45] T. Huang, C. Wang, H. Yu, H. Wang, Q. Zhang, M. Zhu, *Nano Energy* **2014**, *14*, 226.
[46] P. Huang, D. L. Wen, Y. Qiu, M. H. Yang, C. Tu, H. S. Zhong, X. S. Zhang, *Micromachines* **2021**, *12*, 158.
[47] S. Li, Q. Zhong, J. Zhong, X. Cheng, B. Wang, B. Hu, J. Zhou, *ACS Appl. Mater. Interfaces* **2015**, *7*, 14912.
[48] W. Paosangthong, R. Torah, S. Beeby, *Nano Energy* **2019**, *55*, 401.
[49] Y. C. Lai, J. Deng, S. L. Zhang, S. Niu, H. Guo, Z. L. Wang, *Adv. Funct. Mater.* **2017**, *27*, 1604462.
[50] T. Huang, J. Zhang, B. Yu, H. Yu, H. Long, H. Wang, Q. Zhang, M. Zhu, *Nano Energy* **2019**, *58*, 375.
[51] J. Chen, H. Guo, X. Pu, X. Wang, Y. Xi, C. Hu, *Nano Energy* **2018**, *50*, 536.
[52] W. Paosangthong, M. Wagih, R. Torah, S. Beeby, *Nano Energy* **2022**, *92*, 106739.
[53] S. S. Kwak, H. J. Yoon, S. W. Kim, *Adv. Funct. Mater.* **2019**, *29*, 1804533.
[54] L. B. Huang, G. Bai, M. C. Wong, Z. Yang, W. Xu, J. Hao, *Adv. Mater.* **2016**, *28*, 2744.
[55] Y. Zi, J. Wang, S. Wang, S. Li, Z. Wen, H. Guo, Z. L. Wang, *Nat. Commun.* **2016**, *7*, 10987.
[56] D. A. Winter, *Biomechanics and Motor Control of Human Movement*, John Wiley & Sons, Hoboken, New Jersey, US **2009**.
[57] B. Yang, Y. Xiong, K. Ma, S. Liu, X. Tao, *EcoMat* **2020**, *2*, 12054.
[58] R. Riemer, A. Shapiro, *J. NeuroEng. Rehabil.* **2011**, *8*, 1.

[59] M. He, W. Du, Y. Feng, S. Li, W. Wang, X. Zhang, A. Yu, L. Wan, J. Zhai, *Nano Energy* **2021**, *86*, 106058.
[60] S. Wang, L. Lin, Z. L. Wang, *Nano Energy* **2015**, *11*, 436.
[61] X. S. Zhang, M. D. Han, B. Meng, H. X. Zhang, *Nano Energy* **2015**, *11*, 304.
[62] K. Dong, Y. Hu, J. Yang, S. W. Kim, W. Hu, Z. L. Wang, *MRS Bull.* **2021**, *46*, 512.
[63] X. Pu, C. Zhang, Z. L. Wang, *Natl. Sci. Rev.* **2023**, *10*, nwac170.
[64] R. D. I. G. Dharmasena, J. H. B. Deane, S. R. P. Silva, *Adv. Energy Mater.* **2018**, *8*, 1802190.
[65] K. Dong, X. Peng, R. Cheng, C. Ning, Y. Jiang, Y. Zhang, Z. L. Wang, *Adv. Mater.* **2022**, *34*, 2109355.
[66] K. Dong, Z. L. Wang, *J. Semicond.* **2021**, *42*, 101601.
[67] C. Ning, G. Zheng, K. Dong, *Adv. Sens. Res.* **2023**, *2*, 2200044.
[68] A. Sayam, F. Rabbi, M. Hossain, O. Faruque, N. Ahmed, S. Alimuzzaman, F. Ahmed, R. Islam, A. N. M. M. Rahman, *J. Nat. Fibers* **2021**, *19*, 8923.
[69] R. H. Gong, B. Ozgen, M. Soleimani, *Text. Res. J.* **2009**, *79*, 1014.
[70] C. M. Lin, C. W. Lou, J. H. Lin, *Text. Res. J.* **2009**, *79*, 993.
[71] K. Bilisik, *Text. Res. J.* **2013**, *83*, 1414.
[72] T. M. Dip, A. S. Emu, M. N. H. Nafiz, P. Kundu, H. R. Rakhi, A. Sayam, M. Akhtarujjman, M. Shoaib, M. S. Ahmed, S. T. Ushno, A. I. Asheque, E. Hasnat, M. A. Uddin, A. S. M. Sayem, *Text. Prog.* **2020**, *52*, 167.
[73] Y. Zhu, J. Qin, G. Shi, C. Sun, M. Ingram, S. Qian, J. Lu, S. Zhang, Y. L. Zhong, *Carbon Energy* **2022**, *4*, 1242.
[74] J. Yin, V. S. Reddy, A. Chinnappan, S. Ramakrishna, L. Xu, *Polym. Rev.* **2023**, *63*, 715.
[75] J. Yin, J. Wang, S. Ramakrishna, L. Xu, *ACS Appl. Nano Mater.* **2023**, *6*, 15416.
[76] C. Jiang, C. Wu, X. Li, Y. Yao, L. Lan, F. Zhao, Z. Ye, Y. Ying, J. Ping, *Nano Energy* **2019**, *59*, 268.
[77] N. Gogurla, S. Kim, *Adv. Energy Mater.* **2021**, *11*, 2100801.
[78] J. Yin, J. Li, S. Ramakrishna, L. Xu, *ACS Sustainable Chem. Eng.* **2023**, *11*, 14020.
[79] A. Borode, N. Ahmed, P. Olubambi, *J. Cleaner Prod.* **2019**, *241*, 118311.
[80] J. Gao, K. Shang, Y. Ding, Z. Wen, *J. Mater. Chem. A* **2021**, *9*, 8950.
[81] D. Choi, Y. Lee, Z. H. Lin, S. Cho, M. Kim, C. K. Ao, S. Soh, C. Sohn, C. K. Jeong, J. Lee, M. Lee, *ACS Nano* **2023**, *17*, 11087.
[82] W. Yu, L. Sisi, Y. Haiyan, L. Jie, *RSC Adv.* **2020**, *10*, 15328.
[83] A. Ali, P. K. Shen, *Carbon Energy* **2020**, *2*, 99.
[84] A. K. Geim, K. S. Novoselov, *Nat. Mater.* **2007**, *6*, 183.
[85] C. Lee, X. Wei, J. W. Kysar, J. Hone, *Science* **2008**, *321*, 385.
[86] S. K. Tiwari, S. Sahoo, N. Wang, A. Huczko, *J. Sci.: Adv. Mater. Devices* **2020**, *5*, 10.
[87] F. De Juan, A. Cortijo, M. A. H. Vozmediano, A. Cano, *Nat. Phys.* **2011**, *7*, 810.
[88] H. Ahmad, M. Fan, D. Hui, *Composites, Part B* **2018**, *145*, 270.
[89] Q. Guo, N. Chen, L. Qu, *Carbon Energy* **2020**, *2*, 54.
[90] V. Harnchana, H. V. Ngoc, W. He, A. Rasheed, H. Park, V. Amornkitbamrung, D. J. Kang, *ACS Appl. Mater. Interfaces* **2018**, *10*, 25263.
[91] S. Choi, C. Kim, J. M. Suh, H. W. Jang, *Carbon Energy* **2019**, *1*, 85.
[92] S. V. Tkachev, E. Y. Buslaeva, A. V. Naumkin, S. L. Kotova, I. V. Laure, S. P. Gubin, *Inorg. Mater.* **2012**, *48*, 796.
[93] H. Jiang, H. Lei, Z. Wen, J. Shi, D. Bao, C. Chen, J. Jiang, Q. Guan, X. Sun, S. T. Lee, *Nano Energy* **2020**, *75*, 105011.
[94] C. Jeong, C. Joung, S. Lee, M. Q. Feng, Y. B. Park, *Int. J. Precis. Eng. Manuf. Technol.* **2020**, *7*, 247.
[95] A. M. Hassanien, A. A. Atta, A. A. Ward, E. M. Ahmed, A. Alsubaie, M. M. El-Nahass, T. Altalhi, *Mater. Res. Express* **2019**, *6*, 125304.
[96] M. E. Turan, Y. Sun, Y. Akgul, *J. Alloys Compd.* **2018**, *740*, 1149.
[97] P. Tian, L. Tang, K. S. Teng, S. P. Lau, *Mater. Today Chem.* **2018**, *10*, 221.
[98] Y. Liu, J. Ping, Y. Ying, *Adv. Funct. Mater.* **2021**, *31*, 2009994.
[99] Y. Gao, G. Liu, T. Bu, Y. Qi, Y. Xie, S. Xu, W. Deng, W. Yang, C. Zhang, *Nano Res.* **2021**, *14*, 4833.
[100] C. Jiang, X. Li, Y. Yao, L. Lan, Y. Shao, F. Zhao, Y. Ying, J. Ping, *Nano Energy* **2019**, *66*, 104121.
[101] T. Bhatta, P. Maharjan, H. Cho, C. Park, S. H. Yoon, S. Sharma, M. Salauddin, M. T. Rahman, S. M. S. Rana, J. Y. Park, *Nano Energy* **2021**, *81*, 105670.
[102] S. Bayan, S. Pal, S. K. Ray, *Nano Energy* **2022**, *94*, 106928.
[103] C. H. Park, J. K. Park, H. S. Jeon, B. C. Chun, *J. Electrostat.* **2008**, *66*, 578.
[104] H. Zou, Y. Zhang, L. Guo, P. Wang, X. He, G. Dai, H. Zheng, C. Chen, A. C. Wang, C. Xu, Z. L. Wang, *Nat. Commun.* **2019**, *10*, 1427.
[105] F. F. Hatta, M. A. S. M. Haniff, M. A. A. Mohamed, *Int. J. Energy Res.* **2022**, *46*, 544.
[106] S. Liu, W. Zheng, B. Yang, X. Tao, *Nano Energy* **2018**, *53*, 383.
[107] B. Zhang, J. Lei, D. Qi, Z. Liu, Y. Wang, G. Xiao, J. Wu, W. Zhang, F. Huo, X. Chen, *Adv. Funct. Mater.* **2018**, *28*, 1801683.
[108] S. Niu, S. Wang, L. Lin, Y. Liu, Y. S. Zhou, Y. Hua, Z. L. Wang, *Energy Environ. Sci.* **2013**, *6*, 3576.
[109] V. Kaushik, J. Lee, J. Hong, S. Lee, S. Lee, J. Seo, C. Mahata, T. Lee, *Nanomaterials* **2015**, *5*, 1493.
[110] Y. Li, W. Zheng, H. Zhang, H. Wang, H. Cai, Y. Zhang, Z. Yang, *Nano Energy* **2020**, *70*, 104540.
[111] H. Chu, H. Jang, Y. Lee, Y. Chae, J. H. Ahn, *Nano Energy* **2016**, *27*, 298.
[112] C. Chen, L. Zhang, W. Ding, L. Chen, J. Liu, Z. Du, W. Yu, *Energies* **2020**, *13*, 4119.
[113] W. Sun, Z. Ding, Z. Qin, F. Chu, Q. Han, *Nano Energy* **2020**, *70*, 104526.
[114] M. G. Stanford, J. T. Li, Y. Chyan, Z. Wang, W. Wang, J. M. Tour, *ACS Nano* **2019**, *13*, 7166.
[115] M. G. Stanford, C. Zhang, J. D. Fowlkes, A. Hoffman, I. N. Ivanov, P. D. Rack, J. M. Tou, *ACS Appl. Mater. Interfaces* **2020**, *12*, 10902.
[116] J. Wang, C. Lu, K. Zhang, *Energy Environ. Mater.* **2020**, *3*, 80.
[117] J. Han, C. Xu, J. Zhang, N. Xu, Y. Xiong, X. Cao, Y. Liang, L. Zheng, J. Sun, J. Zhai, Q. Sun, Z. L. Wang, *ACS Nano* **2021**, *15*, 1597.
[118] J. Zhong, Y. Zhang, Q. Zhong, Q. Hu, B. Hu, Z. L. Wang, J. Zhou, *ACS Nano* **2014**, *8*, 6273.
[119] K. N. Kim, J. Chun, J. W. Kim, K. Y. Lee, J. U. Park, S. W. Kim, Z. L. Wang, J. M. Baik, *ACS Nano* **2015**, *9*, 6394.
[120] Y. Yang, L. Xie, Z. Wen, C. Chen, X. Chen, A. Wei, P. Cheng, X. Xie, X. Sun, *ACS Appl. Mater. Interfaces* **2018**, *10*, 42356.
[121] M. Zhang, M. Zhao, M. Jian, C. Wang, A. Yu, Z. Yin, X. Liang, H. Wang, K. Xia, X. Liang, J. Zhai, Y. Zhang, *Matter* **2019**, *1*, 168.
[122] X. Yu, J. Pan, J. Zhang, H. Sun, S. He, L. Qiu, H. Lou, X. Sun, H. Peng, *J. Mater. Chem. A* **2017**, *5*, 6032.
[123] W. J. Kim, S. Cho, J. Hong, J. P. Hong, *Compos. Sci. Technol.* **2022**, *219*, 109247.
[124] L. Yan, Y. Mi, Y. Lu, Q. Qin, X. Wang, J. Meng, F. Liu, N. Wang, X. Cao, *Nano Energy* **2022**, *96*, 107135.
[125] Z. Li, B. Xu, J. Han, J. Huang, H. A. Fu, *Adv. Funct. Mater.* **2022**, *32*, 2106731.
[126] Y. Chen, Z. Deng, R. Ouyang, R. Zheng, Z. Jiang, H. Bai, H. Xue, *Nano Energy* **2021**, *84*, 105866.
[127] H. J. Sim, C. Choi, S. H. Kim, K. M. Kim, C. J. Lee, Y. T. Kim, X. Lepró, R. H. Baughman, S. J. Kim, *Sci. Rep.* **2016**, *6*, 35153.
[128] H. Chen, W. Yang, C. Zhang, M. Wu, W. Li, Y. Zou, L. Lv, H. Yu, H. Ke, R. Liu, Y. Xu, J. Wang, Z. Li, *Nano Res.* **2022**, *15*, 2465.
[129] Z. Qin, Y. Yin, W. Zhang, C. Li, K. Pan, *ACS Appl. Mater. Interfaces* **2019**, *11*, 12452.

[130] H. Chen, Y. Xu, J. Zhang, W. Wu, G. Song, *Nano Energy* **2019**, *58*, 304.
[131] K. Xia, D. Wu, J. Fu, N. A. Hoque, Y. Ye, Z. Xu, *J. Mater. Chem. A* **2020**, *8*, 25995.
[132] B. N. Chandrashekar, B. Deng, A. S. Smitha, Y. Chen, C. Tan, H. Zhang, H. Peng, Z. Liu, *Adv. Mater.* **2015**, *27*, 5210.
[133] X. He, Y. Zi, H. Geo, H. Zheng, Y. Xi, C. Wu, J. Wang, W. Zhang, C. Lu, Z. L. Wang, *Adv. Funct. Mater.* **2016**, *27*, 1604378.
[134] J. Wang, S. Li, F. Yi, Y. Zi, J. Lin, X. Wang, Y. Xu, Z. L. Wang, *Nat. Commun.* **2016**, *7*, 12744.
[135] Z. Bai, T. He, Z. Zhang, Y. Xu, Z. Zhang, Q. Shi, Y. Yang, B. Zhou, M. Zhu, J. Guo, C. Lee, *Nano Energy* **2022**, *94*, 106956.
[136] J. Kim, W. Kim, G. Jang, D. S. Hyeon, M. H. Park, J. P. Hong, *Adv. Energy Mater.* **2020**, *10*, 1903217.
[137] M. Su, B. Kim, *ACS Appl. Nano Mater.* **2020**, *3*, 9759.
[138] C. Wu, T. W. Kim, F. Li, T. Guo, *ACS Nano* **2016**, *10*, 6449.
[139] S. Hu, J. Han, Z. Shi, K. Chen, N. Xu, Y. Wang, R. Zheng, Y. Tao, Q. Sun, Z. L. Wang, G. Yang, *Nano-Micro Lett.* **2022**, *14*, 115.
[140] P. Zhang, W. Zhang, A. Zhang, *Energy Technol. Assess.* **2021**, *46*, 101290.
[141] M. Shi, H. Wu, J. Zhang, M. Han, B. Meng, H. Zhang, *Nano Energy* **2017**, *32*, 479.
[142] R. Cao, X. Pu, X. Du, W. Yang, J. Wang, H. Guo, S. Zhao, Z. Yuan, C. Zhang, C. Li, Z. L. Wang, *ACS Nano* **2018**, *12*, 5190.
[143] P. Feng, Z. Xia, B. Sun, X. Jing, H. Li, X. Tao, H. Y. Mi, Y. Liu, *Appl. Mater. Interfaces* **2021**, *13*, 16916.
[144] L. Liu, J. Pan, P. Chen, J. Zhang, X. Yu, X. Ding, B. Wang, X. Sun, H. Peng, *J. Mater. Chem. A* **2016**, *4*, 6077.
[145] Z. Bai, Z. Zhang, J. Li, J. Guo, *Nano Energy* **2019**, *65*, 104012.
[146] R. Wu, L. Ma, A. Patil, Z. Meng, S. Liu, C. Hou, Y. Zhang, W. Yu, W. Guo, X. Y. Liu, *J. Mater. Chem. A* **2020**, *8*, 12665.
[147] Y. Mao, Y. Li, J. Xie, C. Guo, W. Hu, *Nano Energy* **2021**, *84*, 105918.
[148] F. Xu, S. Dong, G. Liu, C. Pan, Z. H. Guo, W. Guo, L. Li, Y. Liu, C. Zhang, X. Pu, Z. L. Wang, *Nano Energy* **2021**, *88*, 106247.
[149] E. He, Y. Sun, X. Wang, H. Chen, B. Sun, B. Gu, W. Zhang, *Composites, Part B* **2020**, *200*, 108244.
[150] C. J. Lee, A. Y. Choi, C. Choi, H. J. Sim, S. J. Kim, Y. T. Kim, *RSC Adv.* **2016**, *6*, 10094.
[151] M. Zhu, Y. Huang, W. S. Ng, J. Liu, Z. Wang, Z. Wang, H. Hu, C. Zhi, *Nano Energy* **2016**, *27*, 439.
[152] C. Zhou, Y. Yang, N. Shun, Z. Wen, P. Cheng, X. Xie, H. Shao, Q. Shen, X. Chen, Y. Liu, Z. L. Wang, X. Sun, *Nano Res.* **2018**, *11*, 4313.
[153] Y. Guo, X. S. Zhang, Y. Wang, W. Gong, Q. Zhang, H. Wang, J. Brugger, *Nano Energy* **2018**, *48*, 152.
[154] M. Su, J. Brugger, B. Kim, *Int. J. Precis. Eng. Manuf. Green Technol.* **2020**, *7*, 683.
[155] J. Xiong, T. Huang, H. Zuo, S. Qian, Y. Guo, L. Sun, D. Lei, Q. Wu, B. Zhu, C. He, X. Mo, E. Jeffries, H. Yu, Z. You, *Nat. Commun.* **2018**, *28*, 1805108.
[156] D. L. Wen, X. Liu, H. T. Deng, D. H. Sun, H. Y. Qian, J. Brugger, X. S. Zhang, *Nano Energy* **2019**, *66*, 104123.
[157] Y. Song, J. Zhang, H. Guo, X. Chen, Z. Su, H. Chen, X. Cheng, H. Zhang, *Appl. Phys. Lett.* **2017**, *111*, 073901.
[158] A. R. Mule, B. Dudem, S. A. Graham, J. S. Yu, *Adv. Funct. Mater.* **2019**, *29*, 1807779.
[159] X. Xia, J. Chen, G. Liu, M. S. Javed, X. Wang, C. Hu, *Carbon* **2017**, *111*, 569.
[160] X. Ding, H. Cao, K. Zhang, M. Li, Y. Liu, *Sensors* **2018**, *18*, 1713.
[161] T. Zhao, J. Li, H. Zeng, Y. Fu, H. He, L. Xing, Y. Zhang, X. Xue, *Nanotechnology* **2018**, *29*, 405504.
[162] H. Wang, Y. Yu, X. Yang, S. Wang, J. Ge, Q. Yang, X. Zhou, G. Zheng, K. Dai, X. Dai, Y. Feng, *EcoMat* **2023**, *5*, 12337.
[163] G. Zhu, Y. Sheng Zhou, P. Bai, X. S. Meng, Q. Jing, J. Chen, Z. L. Wang, *Adv. Mater.* **2014**, *26*, 3788.
[164] S. Chamanian, B. Çiftci, H. Uluşan, A. Muhtaroğlu, H. Külah, *IEEE Trans. Circuits Syst. I Regul. Pap.* **2019**, *66*, 2784.
[165] Y. Xie, S. Wang, S. Niu, L. Lin, Q. Jing, J. Yang, Z. Wu, Z. L. Wang, *Adv. Mater.* **2014**, *26*, 6599.
[166] X. Cheng, W. Tang, Y. Song, H. Chen, H. Zhang, Z. L. Wang, *Nano Energy* **2019**, *61*, 517.
[167] T. L. Andrew, L. Zhang, N. Cheng, M. Baima, J. J. Kim, L. Allison, S. Hoxie, *Acc. Chem. Res.* **2018**, *51*, 850.
[168] A. Y. Choi, C. J. Lee, J. Park, D. Kim, Y. T. Kim, *Sci. Rep.* **2017**, *7*, 45583.
[169] Q. Qiu, M. Zhu, Z. Li, K. Qiu, X. Liu, J. Yu, B. Ding, *Nano Energy* **2019**, *58*, 750.
[170] S. Park, M. Vosguerichian, Z. Bao, *Nanoscale* **2013**, *5*, 1727.
[171] W. Yan, C. Dong, Y. Xiang, S. Jiang, A. Leber, G. Loke, W. Xu, C. Hou, S. Zhou, M. Chen, R. Hu, P. P. Shun, L. Wei, X. Jia, F. Sorin, X. Tao, G. Tao, *Mater. Today* **2020**, *35*, 168.
[172] A. Dixit, H. S. Mali, *Mech. Compos. Mater.* **2013**, *49*, 1.
[173] A. Yu, X. Pu, R. Wen, M. Liu, T. Zhou, K. Zhang, Y. Zhang, J. Zhai, W. Hu, Z. L. Wang, *ACS Nano* **2017**, *11*, 12764.
[174] J. Shi, S. Liu, L. Zhang, B. Yang, L. Shu, Y. Yang, M. Ren, Y. Wang, J. Chen, W. Chen, Y. Chai, X. Tao, *Adv. Mater.* **2020**, *32*, 1901958.
[175] V. Nguyen, R. Zhu, R. Yang, *Nano Energy* **2015**, *14*, 49.
[176] Y. Lee, S. H. Cha, Y. W. Kim, D. Choi, J. Y. Sun, *Nat. Commun.* **2018**, *9*, 1804.
[177] K. Winands, K. Müller, C. Kollera, T. A. Gries, *J. Prod. Syst. Logist.* **2022**, *2*, 1.
[178] Z. Hou, X. Liu, M. Tian, X. Zhang, L. Qu, T. Fan, J. Miao, *J. Mater. Chem. A* **2023**, *11*, 17336.
[179] M. Zhu, Q. Shi, T. He, Z. Yi, Y. Ma, B. Yang, T. Chen, C. Lee, *ACS Nano* **2019**, *13*, 1940.
[180] R. S. Dey, T. Purkait, N. Kamboj, M. Das, *Carbonaceous Materials and Future Energy: Clean and Renewable Energy Sources*, Taylor & Francis, UK **2019**.
[181] X. Tao, *Acc. Chem. Res.* **2019**, *52*, 307.
[182] A. H. Khadem, *Adv. Mater. Interfaces* **2024**, *11*, 2300724.
[183] K. Chatterjee, T. K. Ghosh, *Adv. Mater.* **2020**, *32*, 1902086.
[184] S. Hong, J. Lee, K. Do, M. Lee, J. H. Kim, S. Lee, D. H. Kim, *Adv. Funct. Mater.* **2017**, *27*, 1704353.
[185] P. Gljušćić, S. Zelenika, D. Blažević, E. Kamenar, *Sensors* **2019**, *19*, 4922.
[186] X. Liu, X. Liu, T. Chen, F. Qian, Z. Guo, F. X. Lin, X. Wang, K. Chen, in *MobiSys'17: Proc. 15th Annual Int. Conf. Mobile Systems, Applications, and Services*, USA **2017**, p. 385.
[187] S. Bairagi, C. Kumar, A. Babu, A. K. Aliyana, G. Stylios, S. C. Pillai, D. M. Mulvihill, *Nano Energy* **2023**, *118*, 108962.
[188] M. P. Mahmud, A. Zolfagharian, S. Gharaie, A. Kaynak, S. H. Farjana, A. V. Ellis, J. Chen, A. Z. Kouzani, *Adv. Energy Sustainability Res.* **2021**, *2*, 99.
[189] A. Sayam, A. N. M. M. Rahman, M. S. Rahman, S. A. Smriti, F. Ahmed, M. F. Rabbi, M. Hossain, M. O. Faruque, *Carbon Lett.* **2022**, *32*, 1173.
[190] J. Xu, W. Zhong, W. Yao, *J. Mater. Sci.* **2010**, *45*, 3538.
[191] A. Lekawa-Raus, J. Patmore, L. Kurzepa, J. Bulmer, K. Koziol, *Adv. Funct. Mater.* **2014**, *24*, 3661.
[192] A. N. Sruti, K. Jagannadham, *J. Electron. Mater.* **2010**, *39*, 1268.
[193] L. Chen, X. Yin, X. Fan, M. Chen, X. Ma, L. Cheng, L. Zhang, *Carbon* **2015**, *95*, 10.
[194] V. B. Mohan, R. Brown, K. Jayaraman, D. Bhattacharyya, *Mater. Sci. Eng., B* **2015**, *193*, 49.

[195] R. M. Always-Cooper, D. P. Anderson, A. A. Ogale, *Carbon* **2013**, *59*, 40.
[196] R. Sanjinés, M. D. Abad, C. Vâju, R. Smajda, M. Mionić, A. Magrez, *Surf. Coat. Technol.* **2011**, *206*, 727.
[197] Z. Li, M. Zhu, Q. Qiu, J. Yu, B. Ding, *Nano Energy* **2018**, *53*, 726.
[198] C. Ning, K. Dong, R. Cheng, J. Yi, C. Ye, X. Peng, F. Sheng, Y. Jiang, Z. L. Wang, *Adv. Funct. Mater.* **2020**, *31*, 2006679.
[199] Q. Guan, G. Lin, Y. Gong, J. Wang, W. Tan, D. Bao, Y. Liu, Z. You, X. Sun, Z. Wen, Y. Pan, *J. Mater. Chem. A* **2019**, *7*, 13948.
[200] Y. Jin, D. Ka, S. Jang, D. Heo, J. A. Seo, H. Jung, K. Jeong, S. Lee, *Nanomaterials* **2021**, *11*, 940.
[201] H. Guo, T. Li, X. Cao, J. Xiong, Y. Jie, M. Willander, X. Cao, N. Wang, Z. L. Wang, *ACS Nano* **2017**, *11*, 856.
[202] I. J. Chung, W. Kim, W. Jang, H. W. Park, A. Sohn, K. B. Chung, D. W. Kim, D. Choi, Y. T. Park, *J. Mater. Chem. A* **2018**, *6*, 3108.
[203] G. Pace, A. Ansaldo, M. Serri, S. Lauciello, F. Bonaccorso, *Nano Energy* **2020**, *76*, 104989.
[204] M. S. Rasel, H. O. Cho, J. W. Kim, J. Y. Park, *J. Phys.: Conf. Ser.* **2018**, *1052*, 012029.
[205] H. Chen, L. Miao, Z. Su, Y. Song, M. Han, X. Chen, X. Cheng, D. Chen, H. Zhang, *Nano Energy* **2017**, *40*, 65.
[206] S. Chen, T. Huang, H. Zuo, S. Qian, Y. Guo, L. Sun, D. Lei, Q. Wu, B. Zhu, C. He, X. Mo, E. Jeffries, H. Yu, Z. You, *Adv. Funct. Mater.* **2018**, *28*, 1805108.
[207] M. O. Shaikh, Y. B. Huang, C. C. Wang, C. H. Chuang, *Micromachines* **2019**, *10*, 438.

Abdullah Sayam is currently a lecturer in the Department of Textile Engineering, Ahsanullah University of Science & Technology. He earned his B.Sc. degree in textile engineering from the Bangladesh University of Textiles with a specialization in fabric manufacturing. His research interests are focused on energy conversion and storage-based power wearables, 3D printing, and carbon-based composite materials.

Mahfuzur Rahman graduated from Bangladesh University of Textiles (BUTEX), specializing in industrial and production engineering. His research interests include nanomaterials and nanomechanics, magnetic materials, wearable smart textiles, biomedical applications, thin film magnetism, first-principle DFT studies, and engineered 2D quantum materials. He has previously conducted research on ferrite nanomaterials, synthesizing and characterizing their properties, as well as sustainable textiles. He has recently been working on smart textiles and experimental and DFT analysis of perovskite materials.

Abu Sadat Muhammad Sayem is the lead of the AHRC Digital Fashion Network project hosted at the Manchester Metropolitan University, UK. He is a fellow of the Higher Education Academy, England, Textile institute and Royal Society of Arts. With over 20 years of professional experience, he edits the "Textile Institute Professional Publication Series." He supervised three successful Ph.D. projects and is currently supervising two more. He has been working as a Ph.D. examiner for the Cranfield University since 2020. He chairs the scientific events—Digital Fashion Innovation Conference and the iCongress Innovation Festival.

A. T. M. Faiz Ahmed is currently an associate professor at Bangladesh University of Textiles. His research interests include sustainable materials, technical textiles, and application of computer in textile manufacturing. Dr. Faiz completed his B.Sc. in textile technology from College of Textile Engineering and Technology under the University of Dhaka in 2005. He earned his M.Sc. in technical textiles from University of Bolton, UK in 2013 and gained his Ph.D. from the Department of Textile Sciences and Engineering at Çukurova University, Adana, Turkey.

Shah Alimuzzaman Belal completed his B.Sc. in textile technology from College of Textile Engineering and Technology under the University of Dhaka. He obtained his M.Sc. in textile engineering from University of Ghent, Belgium and completed his Ph.D. from University of Manchester, UK in Textile Science and Technology. He is now working as Vice-Chancellor of Bangladesh University of Textiles. Dr. Shah Alimuzzaman Belal works mainly in the area of knitting, smart textiles, and sustainability in textiles sector.